GEOLOGICAL SURVEY OF CANADA
COMMISSION GÉOLOGIQUE DU CANADA

PAPER 78-16

COMPUTATION OF SYNTHETIC SEISMOGRAMS FOR MARINE REFRACTION STUDIES

C.E. KEEN

Energy, Mines and Resources Canada
Énergie, Mines et Ressources Canada

1978

GEOLOGICAL SURVEY
PAPER 78-16

COMPUTATION OF SYNTHETIC SEISMOGRAMS FOR MARINE REFRACTION STUDIES

C.E. KEEN

1978

available by mail from

Printing and Publishing
Supply and Services Canada,
Hull, Québec, Canada K1A 0S9,

and

The Geological Survey of Canada
601 Booth St., Ottawa, K1A 0E8

or

Through your bookseller.

Catalogue No. M44-78/16 Price: Canada: $2.50
ISBN - 0-660-10120-3 Other Countries: $3.00

Price subject to change without notice

CONTENTS

Tables

Illustrations

Critical readers

D.L. Barrett
M.J. Keen

Author's address

Atlantic Geoscience Centre,
Bedford Institute of Oceanography,
Dartmouth, Nova Scotia

Original manuscript submitted: 1977 - 12 - 22
Approved for publication: 1978 - 1 - 9

COMPUTATION OF SYNTHETIC SEISMOGRAMS FOR MARINE REFRACTION STUDIES

Abstract

A method for calculating synthetic seismograms is presented which can be used for comparing real seismic refraction data obtained with ocean bottom seismometers with that computed for an assumed earth model. The model consists of flat-lying, homogeneous, elastic layers overlain by a fluid half-space. The thickness, P and S wave velocities, density, and specific attenuation factors are specified for each layer. The source is an explosion within the fluid whose detonation depth and size are known. The method involves the calculation of the generalized plane wave reflection coefficients for the structure at different angles of incidence and frequencies. These coefficients then form part of integral expressions for the reflected spherical wave field which are evaluated by numerical quadrature. The use of a computer program for the generation of synthetic seismograms, which correspond to the vertical component of particle velocity at the sea floor and are modified by the frequency response of the recording instruments, is described. Examples of computed seismograms and the specification of numerical parameters used as part of the program input are given.

Résumé

Dans le présent rapport, on présente une méthode de calcul des sismogrammes synthétiques, permettant de comparer les données réelles de sismique-réfraction obtenues à l'aide de sismomètres placés sur le fond de l'océan, avec les résultats de calculs obtenus par modélisation de l'écorce terrestre. Le modèle utilisé consiste en couches élastiques homogènes et planes, recouvertes par un demi-espace fluide. L'épaisseur, la vitesse des ondes P et S, la densité, et les facteurs d'amortissement spécifique sont indiqués pour chaque couche. La source est une explosion dans le fluide choisi, la profondeur et la force de la détonation étant connues. La méthode comprend le calcul des coefficients de réflexion de l'onde plane généralisée, qui caractérisent la structure pour divers angles d'incidence et diverses fréquences. Ces coefficients font alors partie des expressions intégrales applicables au champ d'ondes sphériques réfléchies, expressions que l'on calcule par quadrature numérique. On décrit le mode d'utilisation d'un programme-machine pour la production de sismogrammes synthétiques qui correspondent à la composante verticale de la vitesse des particules sur le fond marin, et sont modifiés par la réponse de fréquence des appareils enregistreurs. On donne des exemples de sismogrammes calculés, et l'on spécifie les paramètres numériques qui ont fait partie de l'entrée de programme.

COMPUTATION OF SYNTHETIC SEISMOGRAMS FOR MARINE REFRACTION STUDIES

INTRODUCTION

Marine seismic refraction techniques have recently been greatly improved by the use of ocean bottom seismometers which have elminated many of the difficulties associated with near surface instruments (Kennett, 1977). These give an improvement in signal-to-noise ratio and the ability to obtain particle motions from horizontal and vertical geophones. The improvement in the data has been accompanied by more advanced techniques of data analysis including better methods for the inversion of travel times and the use of synthetic seismograms, so that a more detailed interpretation of the oceanic crustal structure can be made. In areas of young oceanic crust where most of the new studies have been concentrated, it is now possible to search for low velocity zones in the crust, possibly associated with magma chambers beneath the axial zones of ridge crests (Fowler, 1976; Orcutt et al., 1976) and to investigate the development of the oceanic crust with time (Lewis and Snydsman, 1977).

The Atlantic Geoscience Centre has recently acquired an ocean bottom seismometer system (Barrett et al., 1977) which has been used successfully in refraction experiments over young oceanic crust off the west coast of Canada (Hyndman et al., in press), on the Reykjanes Ridge (Loncarevic, pers. comm.), and on the continental margin northeast of Newfoundland (Keen, 1977). To best use the data from these experiments and future refraction studies a computer program has been developed to generate synthetic seismograms, given as input a sequence of flat-lying homogeneous layers each characterized by P and S velocities and densities, the depth and size of the explosive charge, and the frequency response of the instrument used. The resulting synthetic seismograms can be compared to the observed data and the model adjusted to provide good correspondence between the observed and computed seismograms.

The purpose of this paper is to describe the methods used in the generation of the synthetic seismogram. Many publications outline these methods few give the details of the computational procedures thus allowing the computer program to be used by other investigators. The essence of the ideas presented here follow the reflectivity method of Fuchs and Muller (1971) and Kennett (1974), but the program has been developed specifically for marine refraction interpretation using explosives detonated in water as the source, and seismometers on the ocean floor as the recording devices.

This paper has been organized so that those who wish to use the computer program without much appreciation of the computational methods may turn directly to sections on the use of the computer program where the basic assumptions and directions for the program use are described. The next seven sections outline and review the theory involved in these calculations for readers who wish to obtain an understanding of the techniques. A list of symbols is given in Appendix 1.

Acknowledgments

I would like to thank M. Fowler, B.D. Loncarevic, D. Barrett, D. Porteous, and M. Keen for their help and suggestions in the preparation of this manuscript.

AN OUTLINE OF THE METHOD

The generation of synthetic seismograms can be divided into three parts: (a) specification of the source function, (b) computation of the elastic response of the earth structure chosen, and (c) specification of the characteristics of the recording instrument on the waveforms. I have chosen to work with components of the Fourier spectrum (i.e. to work in the frequency rather than the time domain) so that the total response in the frequency domain can be expressed as $S(\omega) = A(\omega) \cdot E(\omega) \cdot I(\omega)$. Here $S(\omega)$ is the total response which can be transformed to the time domain to give the synthetic seismogram, $S(t) = \int_{-\infty}^{\infty} S(\omega)e^{-i\omega t}d\omega$, and $A(\omega)$, $E(\omega)$, and $I(\omega)$ are the source, earth, and instrument frequency responses.

The geometry of the problem is shown in Figure 1 where a point (explosive) source is detonated a distance, h, below the sea surface and recorded at the sea floor by an ocean bottom seismometer with a horizontal source-receiver separation of r. Below the sea floor, the earth structure is approximated by a number of flat-lying layers and each interface is associated with an index running from i = 1 (sea floor) to i = n (deepest interface). These interfaces occur at $z = z_1 \ldots z_n$. Each layer (for example, the i^{th} layer) is characterized by its P and S wave velocities and density. The first task is to find the form of the compressional wave from the source, incident on the sea floor.

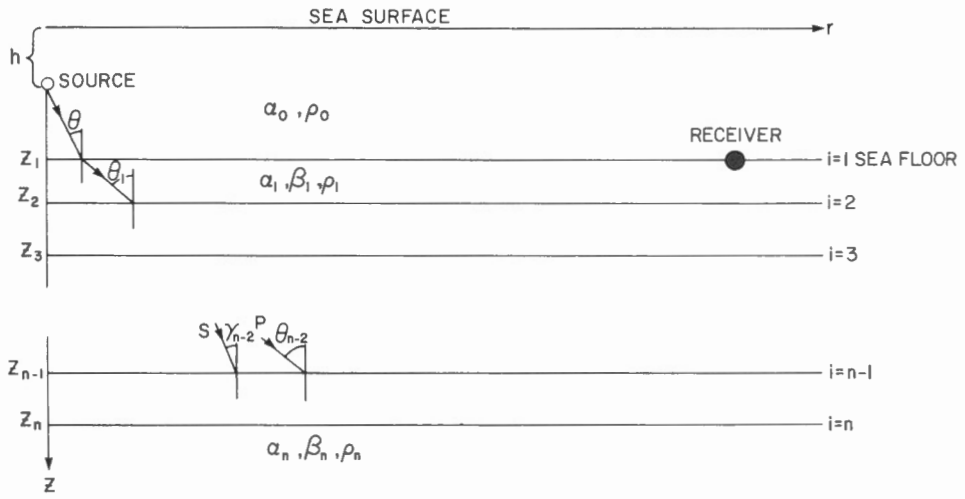

Figure 1. The geometry of the problem, showing the positions of the source and receiver in relation to the layered earth model. Angles θ and γ are the angles of incidence for P and S plane waves respectively. The subscripts refer to the layer in which the wave is propagating. Depths are measured from the sea floor ($z_1 = 0$) and are positive in the downward direction.

The source

The shape of the pressure pulse generated by an explosion is well known (Weston, 1960; Kennett, 1977). It consists of the initial shock wave, followed by a series of bubble pulses caused by the expansion and contraction of gases formed as part of the detonation process. Also, a reflection of each of these pulses from the sea surface occurs at time, $z_t = 2h/\alpha_0$, after the initial pulse. The equations governing the source as a function of detonation depth and charge size are given below and the resulting pressure pulse as a function of time is shown in Figure 2 and Table 1 for a 45 kg (100 lb) charge located 60 m below the sea surface. The detonation time is taken to be t = 0, so that no seismic energy is generated for t < 0. Note that metric units are not used in the equations which follow in order to conform to the units used in the computer program and in most of the literature.

Shock wave: $P = Ps\ e^{-t/Ts} \qquad t \geq 0$

where $Ps = 2.16 \times 10^4\ (W^{1/3}/R)^{1.13}$ lb inch^{-2}

$Ts = 58\ W^{1/3}(W^{1/3}/R)^{-0.22} \times 10^{-6}$ s

and R is the distance from the charge in feet,

W is the charge size in pounds.

First bubble pulse:

$$P = P_{b_1} e^{-(T_1-t)/T_{b_1}} \qquad t \leq T$$

$$= P_{b_1} e^{-(t-T_1)/T_{b_1}} \qquad t \geq T$$

where

$$P_{b_1} = 3450(W^{1/3}/R) \text{ lb inch}^{-2}$$

$$T_{b_1} = 9.58(W^{1/3}/R)(h+33)^{-1/6}/2P_{b_1} \text{ s}$$

$$T_1 = 4.36W^{1/3}(h+33)^{-5/6} \text{ s}$$

Second bubble pulse: This has the same form as the first bubble pulse except some of the energy has been dissipated and therefore the constants have changed as follows:

$$P_{b_2} = P_{b_1}/4.72$$

$$T_{b_2} = 1.91\ T_{b_1}$$

$$T_2 = 0.72\ T_1 + T_1$$

There are more bubble pulses following the second but they contain insignificant energy compared to the first two oscillations and can be ignored.

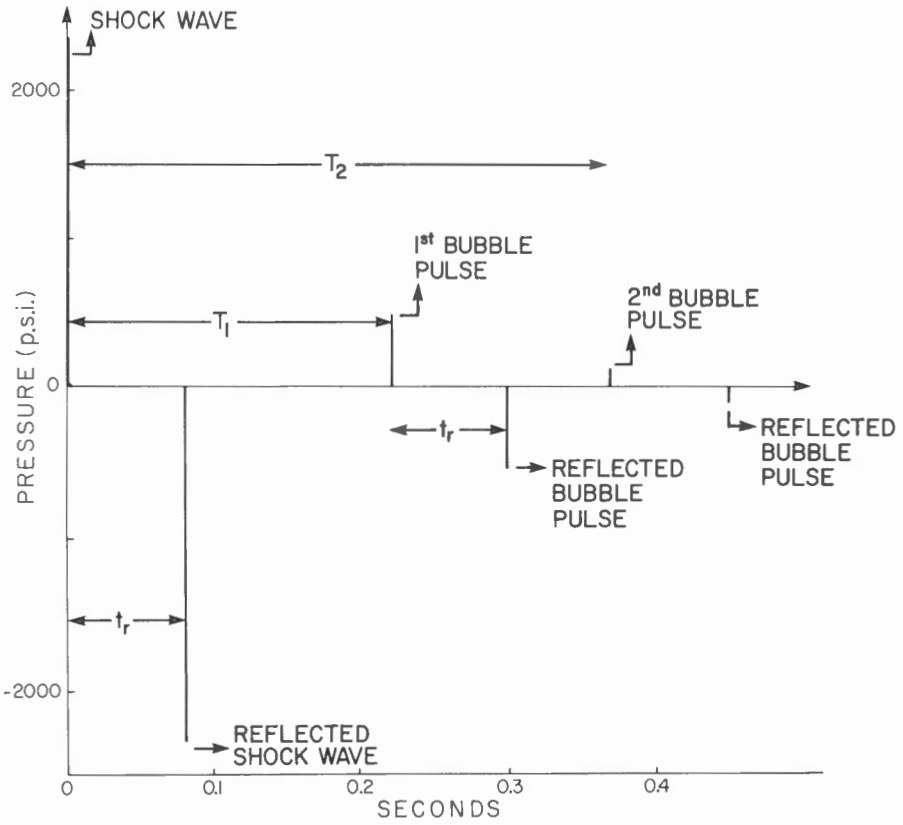

Figure 2. Pressure pulse in water, generated by a 45 kg explosive charge at a depth of 60 m beneath the sea surface and measured at a distance of 10 m. The pulses reflected from the sea surface have been included where t_r is two-way travel time for surface reflections. T_1 and T_2 are the periods of the first and second bubble pulses respectively.

The Fourier Transform $P(\omega)$ of the total pressure response is used. Because the time constants, T_s, T_{b_1} and T_{b_2} are small (about 5×10^{-4} s) compared to the periods of the seismic waves (about 0.1 s) which will be considered, each pulse, the shock wave, and bubble pulses can be treated as an impulse with a flat response over the frequency range of interest (5 to 20 Hz). Hence the Fourier Transform of the pressure source function $P(\omega)$ becomes:

$$P(\omega) = \int_{-\infty}^{\infty} P(t) e^{i\omega t} dt$$

$$= \left[PsTs + 2P_{b_1} T_{b_1} e^{-i\omega T_1} + 2P_{b_2} T_{b_2} e^{-i\omega T_2} \right] \cdot \left[1 - e^{-i\omega tr} \right] \qquad (1)$$

In equation (1), the first term gives the Fourier Transform of the shock wave and the first and second bubble pulses (delayed by the appropriate phase terms corresponding to times T_1 and T_2). The second term gives the contribution of the surface reflections, where each pulse is inverted and delayed by an amount $t_r = 2h/\alpha_0$.

The wave incident on the first boundary (i = 1, Fig. 1) will be a compressional wave with spherical wavefronts. The wave potential in the liquid upper layer for a single frequency component can be written as:

$$\phi(\omega, R) = A(\omega) \frac{e^{ikR}}{R}$$

where R is the distance from the source. The relationship between pressure and wave potential in a liquid is:

$$P(\omega) = \rho_0 \cdot \frac{\partial p}{\partial t} = -i\omega\rho_0 \phi(\omega, R)$$

Table 1
Parameter for a 100 lb (45 kg) Explosive Charge
Detonated 60 m Below the sea surface and evaluated at a
range R = 10 m

Shock Wave	First Bubble Pulse	Second Bubble Pulse
P_s 2369 psi	P_{b_1} 488 psi	P_{b_2} 103 psi
T_s 4.13×10^{-4} s	T_{b_1} 5.60×10^{-4}s	T_{b_2} 10.7×10^{-4} s
	T_1 0.22 s	T_2 0.37 s
t_r – reflection time from sea surface = $2h/\alpha_0 = 2\times60/1.5\times10^3 = 0.080$ s		

$P(\omega)$ is given by equation 1, where the parameters, Ps, Ts, P_{b_1}, etc., are evaluated at some distance, R = a, from the source. Hence from equation 1,

$$P(\omega) = -i\omega\rho_0 A(\omega)\frac{e^{ika}}{a}$$

If the distance, a, is much less than the wavelengths, $k = 2\pi/\lambda$, then $e^{ika} \simeq 1$ and $A(\omega) = P(\omega)a\ /(-i\omega\rho_0)$.

This gives the amplitude of the incident wave, $A(\omega)$, where $\phi = A(\omega)e^{ikR}/R$, evaluated at a frequency, ω.

Integral representation of the response for a layered earth

The spherical wave incident on the boundary (i = 1) can be made an integral sum of plane waves (Fuchs and Muller, 1971; Brekhovskikh, 1960, p. 237-244).

$$\phi(\omega,r,z) = A\frac{e^{ikR}}{R} = ikA(\omega)\int_\Gamma J_0(krsin\theta)sin\theta e^{ikzcos\theta}d\theta$$

The wave potential can be written in a similar manner, due to waves which have propagated through the layered earth model and arrive at the ocean bottom seismometer. Since the detector is located on the seafloor, both P and S waves will be recorded.

For P waves recorded at the ocean bottom seismometer

$$\phi_R(\omega,r,z) = ikA(\omega)\int_\Gamma Vpp(\omega,\theta)J_0(krsin\theta)sin\theta e^{ik(z_1-h)cos\theta}d\theta$$

and for S waves

$$\psi_R(\omega,r,z) = ikA(\omega)\int_\Gamma Vps(\omega,\theta)J_0(krsin\theta)sin\theta e^{ik(z_1-h)cos\theta}d\theta \qquad (2)$$

In these integral expressions $J_0(krsin\theta)$ is the Bessel Function of zero order, θ is the angle of incidence of a plane wave upon the interface i = 1, and Vpp, Vps are the generalized plane wave reflection coefficients for a P wave incident from the liquid onto the layered earth model, producing reflected P and S waves respectively. They will be discussed in detail later.

The contour of integration, Γ, over angles, θ, is shown in Figure 3. It includes all real angles of incidence from 0 to $\pi/2$. At $\pi/2$ the contour leaves the real θ axis and the integral is evaluated at complex θ where $\theta = \pi/2 - i\alpha$, for α real and positive. This integral is evaluated numerically by simple methods of numerical quadrature. Many authors have described other methods of evaluation which consist of the determination of the contributions due to singularities in $Vpp(\omega,\theta)$ and $Vps(\omega,\theta)$ in the complex θ-plane (Phinney, 1961; Heelan, 1953).

The ocean bottom seismometers measure particle velocities in the vertical or horizontal direction; these velocities are obtained from the displacement potentials using the relationships below (Ewing et al., 1957).

Vertical particle displacement: $u_z = \frac{\partial\phi}{\partial z} - \frac{1}{r}\frac{\partial}{\partial r}\left[r\frac{\partial\psi}{\partial r}\right]$

Horizontal particle displacement: $u_r = \frac{\partial\phi}{\partial r} - \frac{\partial^2\psi}{\partial r\partial z}$

Particle velocities:

$$\dot{u}_z = \frac{\partial u_z}{\partial t} \quad , \quad \dot{u}_r = \frac{\partial u_r}{\partial t}$$

$$\dot{u}_z(\omega,r,z) = i\omega k^2 A(\omega) \int_\Gamma [Vpp(\omega,\theta)\cos\theta - iVps(\omega,\theta)k\sin^2\theta] J_0(kr\sin\theta) e^{ik(z_1-h)\cos\theta} \sin\theta d\theta$$

$$\dot{u}_r(\omega,r,z) = -\omega k^2 A(\omega) \int_\Gamma [Vpp(\omega,\theta) - ikVps(\omega,\theta)\cos\theta] J_1(kr\sin\theta) e^{ik(z_1-h)\cos\theta} \sin^2\theta d\theta$$

In the numerical evaluation of these integrals the asymptotic representation of the Bessel functions, J_0 and J_1, are used because in almost all real problems in marine refraction seismology, $kr\sin\theta \gg 1$ (Fuchs and Muller, 1971). Physically this means that the shot-receiver range is much greater than the horizontal wavelength in the elastic media. Therefore

$$\dot{u}_z(\omega,r,z) = \frac{i\omega k^2 A(\omega) e^{-i(\pi/4)}}{\sqrt{2\pi kr}} \int_\Gamma [Vpp(\omega,\theta)\cos\theta - iVps(\omega,\theta)k\sin^2\theta] e^{ikr\sin\theta + ik(z_1-h)\cos\theta} \cdot \sqrt{\sin\theta}\, d\theta \qquad (3)$$

$$\dot{u}_r(\omega,r\ z) = \frac{+i\omega k^2 A(\omega) e^{-i(\pi/4)}}{\sqrt{2\pi kr}} \int_\Gamma [Vpp(\omega,\theta)\sin\theta - ikVps(\omega,\theta)\cos\theta\sin\theta] e^{ikr\sin\theta + ik(z_1-h)\cos\theta} \cdot \sqrt{\sin\theta}\, d\theta$$

These integral representations for $\dot{u}_z$ and $\dot{u}_r$ are similar; the only differences occur in the terms contained in square brackets involving the generalized plane wave reflection coefficients. Only $\dot{u}_z$ can be found from the computer program now but with some modification, $\dot{u}_r$, the horizontal component, could also be obtained.

The integral expressions are essential to the calculation of the synthetic seismograms. Only in this form can the solution be found by the evaluation of plane wave reflection coefficients which can be easily, if not quickly, calculated. The solution (given in equation (3)) represented as an integral sum of plane waves can also provide some physical insight into the various contributions to the seismogram (Brekhovskikh, 1960, Ch. 4).

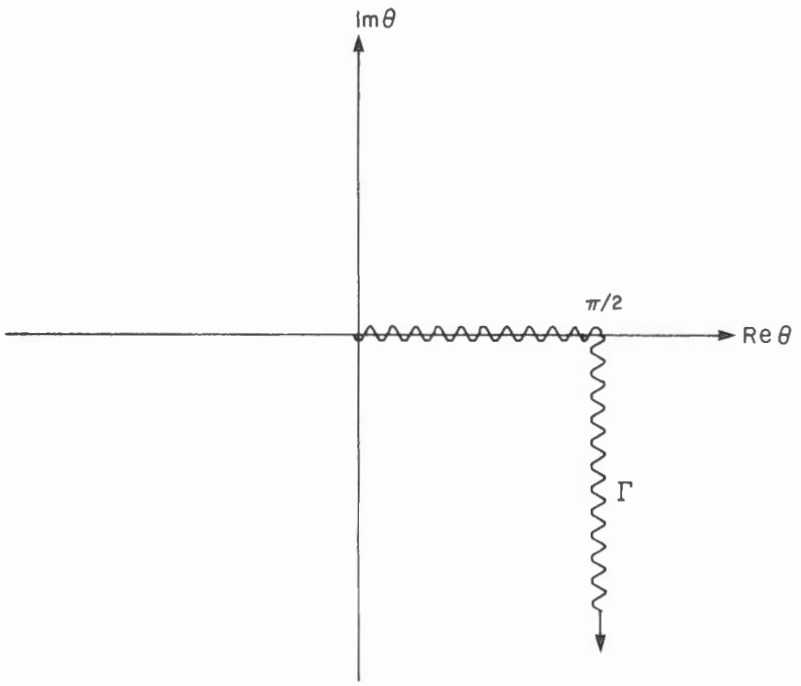

Figure 3. The path of integration, Γ, in the complex θ-plane.

The effect of attenuation

The attenuation of the amplitudes of P and S waves as they travel through the layered earth model can be specified by assigning values for the quality factors, Q_p and Q_s, for P and S waves for each layer. These values range from about 50 for sediments to 500 for crystalline rocks in the lower crust and upper mantle (Knopoff, 1964; Kennett, 1975). The quality factors, Q, are mathematically incorporated into the computations by defining the P and S velocities for each layer as (Kennett, 1975):

$$Vp = Vp\ (1 - i/2Qp),\ V_s = V_s\ (1 - i/2Qs)$$

These modified expressions for velocity lead to exponential decay terms of the form $e^{-(\omega R)/(2VQ)}$. The computer program allows Q_p and Q_s to be specified for each layer and if no attenuation is desired Q_p and Q_s are set equal to zero. [Note that setting Q equal to zero is a computational convenience. The true value of Q is infinity when there is no attenuation.]

Frequency response of the instruments

The frequency bandwidth of the recording instruments usually provides the upper and lower frequency limits of the total seismogram spectrum. Figure 4 shows a typical response curve for instruments used in refraction seismology (Fowler, 1976). Here the response peaks between 5 and 13 Hz and the response can be considered to be zero for frequencies lower than about 1 Hz and higher than about 19 Hz.

The total response is $S(\omega) = A(\omega) \cdot E(\omega) \cdot I(\omega)$. The source times earth response $[A(\omega) \cdot E(\omega)]$ is given by equation (3). For the vertical component of particle motion the total response is given by

$$S(\omega) = \frac{i\omega k^2 A(\omega) I(\omega) e^{\frac{-i\pi}{4}}}{\sqrt{2\pi kr}} \int_\Gamma [Vpp(\omega,\theta)\cos\theta - iVps(\omega,\theta)k\sin^2\theta] e^{ikr\sin\theta + ik(z_1-h)\cos\theta} \sqrt{\sin\theta}\, d\theta \qquad (4)$$

and the synthetic seismogram s(t) is found from:

$$s(t) = \int_{-\infty}^{\infty} S(\omega) e^{-i\omega t} d\omega$$

Hence the synthetic seismogram involves a double integration, over θ and over ω. This is accomplished by finding the integral over θ, for constant ω, and repeating this integration for a set of values of $\omega = \omega_i$. The integral over θ, then, gives us $E(\omega)$ at discrete ω_i and these values are mutiplied by the appropriate $A(\omega_i)$ and $I(\omega_i)$. The values of $A(\omega_i)$ are evaluated using equation 1.

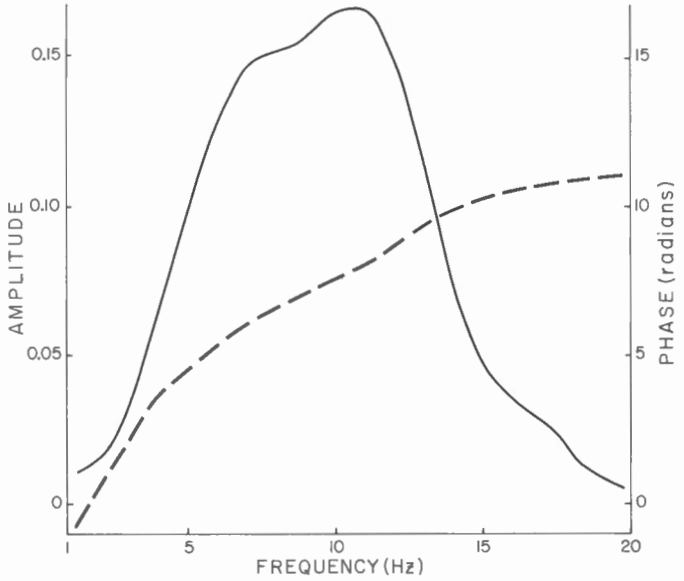

Figure 4. Amplitude and phase response in the frequency domain for typical ocean bottom seismometer recording instruments.

The values of $I(\omega)$ are part of the input to the computer program. This input specifies the frequencies at which $I(\omega)$ are given and these frequencies, ω_0, need not be the same as the frequencies at which the $E(\omega_i)$ are evaluated. Linear interpolation is used between frequencies, ω_0, to obtain the instrument response at any $\omega = \omega_i$. Having found $S(\omega_i)$ the second integration is performed to obtain s(t), the desired synthetic seismogram.

Calculation of the generalized plane wave reflection coefficients, Vpp(ω,θ), Vps(ω,θ)

The calculation of the plane wave reflection coefficients is the most time-consuming and the most difficult part of the problem discussed here. To do this, I have used the method described by Kennett (1974) but because that paper contained a number of important errors, particularly in the appendix, (eqs. 15, 69, 70, 71) the correct form of these equations is presented below and in Appendix 2.

Kennett's (1974) method was based upon the relationships between the reflection coefficients at the i^{th} interface and at the $i\text{-}1^{th}$ interface. At each interface there are 16 possible reflection and transmission coefficients which are listed in Appendix 1. There are four reflection coefficients for plane waves (either P or S) incident from above the $i\text{-}1^{th}$ interface, (see list of symbols for explanation)

$$R_D(z_{i-1}) = \begin{pmatrix} r_{pp}^D & r_{sp}^D \\ r_{ps}^D & r_{ss}^D \end{pmatrix}$$

Similarly there are four reflection coefficients for plane waves incident from below the $i\text{-}1^{th}$ boundary and contained in the matrix $R_U(z_{i-1})$. There are also eight transmission coefficients contained in the two matrices $T_D(z_{i-1})$ and $T_U(z_{i-1})$. As discussed in Appendix 2 these 2x2 matrices are formed from the calculation of the simple plane wave reflection and transmission coefficients at any boundary, i-1, within the layered structure, each of which is multiplied by an appropriate phase term. These phase terms arise because, in the usual reflection and transmission coefficient calculations, the boundary is taken to coincide with the plane z=0, making the phase terms zero also. This is not possible when there is more than one interface – all interfaces cannot lie at z=0. Instead phase terms of the form $e^{-2ikz_{i-1}\cos\theta_{i-1}}$ will multiply the usual form of the plane wave reflection and transmission coefficients. These are called the phase-related reflection and transmission coefficients. Kennett's (1974) relationship between the reflection coefficient at the $i\text{-}1^{th}$ boundary, $V(z_{i-1})$, in terms of the 16 phase-related coefficients corresponding to that boundary and in relation to the reflection coefficient at its i^{th} boundary, $V(z_i)$, is:

$$V(z_{i-1}) = R_D(z_{i-1}) + T_U(z_{i-1})V(z_i)[I - R_U(z_{i-1})V(z_i)]^{-1}T_D(z_{i-1}) \qquad (5)$$

where the complex 2x2 matrices R_D, T_U, R_U, T_D have been discussed above and I is the 2x2 identity matrix. $V(z_{i-1})$ is also a complex 2x2 matrix, each element of which represents one of the four reflection coefficients at the interface z_{i-1}. These are

$$V(z_{i-1}) = \begin{pmatrix} V_{pp}(z_{i-1}) & V_{sp}(z_{i-1}) \\ V_{ps}(z_{i-1}) & V_{ss}(z_{i-1}) \end{pmatrix}$$

where V_{sp}, for example, is the reflection coefficient given by the ratio of the upgoing P wave to the downgoing S wave, at $z = z_{i-1}$ (above the $i\text{-}1^{th}$ interface). Each of these elements includes amplitude and phase terms appropriate to all possible rays propagating in the layered structure below the $i\text{-}1^{th}$ interface. $V(z_i)$ refers to the same quantity calculated for the i^{th} interface.

In order to better understand the physical meaning of equation (5), consider the simple case of a single fluid layer, bounded above ($z = z_{i-1}$) and below ($z = z_i$) by fluid half spaces. Since no S waves propagate in this case, equation (5) becomes a scalar equation; all elements of the 2x2 matrices vanish except for those corresponding to P wave propagation. In addition, let the upper interface at $z = z_{i-1}$ coincide with $z = 0$ and the layer thickness, $h = z_i - z_{i-1}$. Then, as many authors have shown (see, for example Brekhovskikh, 1960), the reflected wave field, related to the plane $z = 0$, can be represented as a sum of ray contributions. These include the reflected

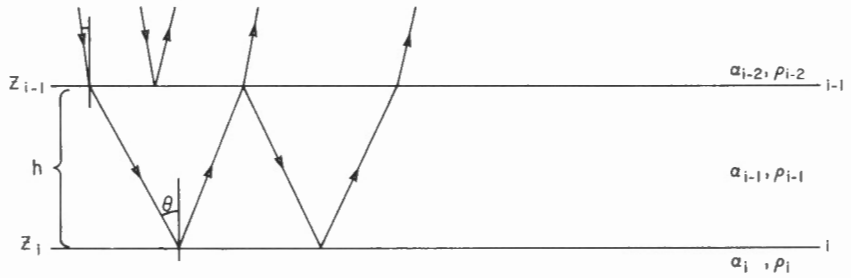

Figure 5. An illustration of some of the more important ray paths of a plane wave incident on the upper boundary of a fluid layer of thickness h. Arrows denote directions of propagation of the rays.

wave from the upper interface, $R_D(z_{j-1})$; the wave transmitted down through the upper interface, reflected from the lower interface, and transmitted up through the upper interface, $T_U(z_{i-1})R_D(z_i)T_D(z_{i-1})$; and multiple reflected waves within the layer (Fig. 5). Represented as a sum of all these contributions the total reflected wave field becomes

$$V(z_{i-1}) = R_D(z_{i-1}) + T_U(z_{i-1})R_D(z_i)T_D(z_{i-1}) \sum_{n=0}^{\infty} [R_D(z_i)R_U(z_{i-1})]^n$$

Here all coefficients related to the boundary $z_{i-1} = 0$ will contain no phase terms; however, $R_D(z_i) = \tilde{R}_D(z_i)e^{2ikh\cos\theta}$ where $\tilde{R}_D$ is the simple downward reflection coefficient at the boundary, i, and the phase term represents propagation in the z direction twice through the layer of thickness h. The equation above can be represented in the equivalent form:

$$V(z_{i-1}) = R_D(z_{i-1}) + T_u(z_{i-1})R_D(z_i)T_D(z_{i-1})[1 - R_D(z_i)R_u(z_{i-1})]^{-1}$$

This is the same as equation (5) for a simple fluid case. The analysis above shows how the generalized plane wave reflection coefficient, $V(z_{i-1})$, contains the effect of all possible ray paths (multiples) within the layer. If the layer is solid, each reflection and transmission coefficient becomes a 2x2 complex matrix and the coefficients, $V(z_{i-1})$, include P-S conversions as well as multiple reflections.

In the case of our layered solid model, equation (5) can be used iteratively to find the generalized reflection coefficient due to a plane P wave or S wave incident on the second interface at angles θ_1 or γ_1 respectively (Fig. 1). The following procedure is adopted:

1. For the deepest interface, i=n, below which there is no reflected energy, calculate the phase-related plane wave reflection coefficients. For this boundary note that $V(z_n) = R_D(z_n)$.
2. Calculate $R_D(z_{n-1})$, $R_U(z_{n-1})$, $T_D(z_{n-1})$, $T_U(z_{n-1})$.
3. Using equaiton (5), calculate $V(z_{n-1})$.
4. Calculate $R_D(z_{n-2})$, $R_U(z_{n-2})$, $T_D(z_{n-2})$, $T_U(z_{n-2})$, and using equation (5), calculate $V(z_{n-2})$.
5. Repeat the process until the interface, i=2, is reached.

Then $V(z_2) = \begin{pmatrix} V_{pp} & V_{sp} \\ V_{ps} & V_{ss} \end{pmatrix}$ will provide the quantities necessary in the evaluation of the integrals (3). It is important to note here that the above process must be repeated for each value of θ at which the integrand of equation (3) is desired and for each frequency ω_i at which the spectrum is needed. The reflection and transmission coefficients at any boundary, i, are found using the relationship between the angle of incidence, θ, on interface 1 and the angle of incidence for P and S waves at any other interface. From Snell's Law (see also Fig. 1)

$$\sin\theta/\alpha_0 = \sin\theta_i/\alpha_{i-1} = \sin\gamma_i/\beta_{i-1}$$

Kennett's (1974) iterative method has been used for the layers below the first layer. Because the source is in the upper fluid and the receiver is on the interface i=1, they must be treated as if they were situated in two different layers and Kennett's method, therefore, does not easily deal with this situation. To circumvent this problem, I assumed that a thin upper layer, usually corresponding to low velocity unconsolidated sediments, be included in the model. This layer can be made as thin as desired and need have no significant effect on the seismograms. The amplitudes of the plane P and S waves transmitted from the water into this layer (corresponding to interface i=1) were calculated by application of the appropriate plane wave transmission coefficients. The iterative equations were used for all interfaces below z_1.

The correspondence between the formulation of equation (5) and the sum of all possible ray contributions to the reflected wave field for a simple fluid case has been shown already. It may be useful, in terms of computation time and for the interpretation of the resulting seismograms in terms of ray theory, to express equation (5) as a partial ray expansion. As was shown for the simple case the term, $[I-R_U(z_{i-1})V(z_i)]^{-1}$, can be written as

$$\{I + \sum_{q=1}^{\infty} [R_u(z_{i-1})V(z_i)]^q\}$$

equation (5) becomes

$$V(z_{i-1}) = R_D(z_{i-1})+T_u(z_{i-1})V(z_i)\{I+ \sum_{q=1}^{\infty} [R_u(z_{i-1})V(z_i)]^q\}T_D(z_{i-1})$$

The series, $\sum_{q=1}^{\infty} [R_U(z_{i-1})V(z_i)]^q$, can be truncated to include only the most important ray paths (Kennett, 1974). If q_{max}, the upper limit of the series, were taken to be 1, equation (5) becomes

$$V(z_{i-1}) = R_D(z_{i-1})+T_u(z_{i-1})V(z_i)T_D(z_{i-1})+T_u(z_{i-1})V(z_i)R_u(z_{i-1})V(z_i)T_D(z_{i-1})$$

The first two terms represent the primary reflections, including P-S conversions, from the upper and lower boundaries and the last term represents the first multiple reflections. Increasing q_{max} will obviously increase the number of multiple reflections allowed. The computer program allows the user to decide upon q_{max} for each layer or allows the complete solution to be calculated.

Numerical integration in the θ-plane

Once the plane wave reflection coefficients, $V_{pp}(\omega,\theta)$ and $V_{ps}(\omega,\theta)$, have been calculated, the integrals (4) must be evaluated numerically. The path of integration, Γ, for integration in the θ plane can be terminated either at $\theta = \pi/2$ or at some real angle $\theta = \theta_{max}$ such that all the ray paths one wishes to consider are included. A lower limit of integration $\theta = \theta_{min}$ may also be specified. The validity of this cutoff is discussed by Fuchs (1968) and by Fuchs and Muller (1971). These terminations can be justified if the source and/or receiver are sufficiently far removed from the nearest boundary that interface waves are not important and if a time window, is considered starting at the first arrival, such that the apparent velocities (c) of all arrivals within that time window satisfy $\alpha_0/\sin\theta_{min} > c = \alpha_0/\sin\theta > \alpha_0/\sin\theta_{max}$. An example is given later.

The numerical quadrature is performed using a modified version of the trapezoidal rule. The integrals (3) in the θ-plane have the form

$$I = \int_{\theta_{min}}^{\theta_{max}} B(\omega,\theta)e^{ik(z_1-h)\cos\theta+ikr\sin\theta}d\theta$$

where $B(\omega,\theta)$ is a function of the plane wave reflection coefficients and can be considered a known function of θ at real values of θ between $\theta = \theta_{min}$ and $\theta = \theta_{max}$. The spacing $\Delta\theta$ at which this evaluation is carried out is an input to the computer program.

The contribution to the integral over each increment $\Delta\theta$ and the sum of all the contributions are used to obtain the value I. Within each increment, $\Delta\theta = \theta_{i+1}-\theta_i$, the complex function $B(\omega,\theta)$ is represented by its amplitude and phase, $B(\omega,\theta) = |B|e^{i\phi}$. The integral over $\Delta\theta$ is

$$\Delta I_i = \int_{\theta_i}^{\theta_{i+1}} |B| e^{i\phi(\theta,\omega)} e^{ik(z_1-h)\cos\theta+ikr\sin\theta}d\theta$$

The total phase term and the amplitude are approximated by straight lines

$$\phi(\theta,\omega) + k(z-h)\cos\theta + kr\sin\theta = m_i\theta + n_i \qquad \theta_i \leq \theta \leq \theta_{i+1}$$

and $$|B(\omega,\theta)| = a_i\theta + b_i$$

Then $$\Delta I_i = \int_{\theta_i}^{\theta_{i+1}} (a_i\theta + b_i)e^{im_i\theta + n_i}\, d\theta$$

$$= \frac{-i\Delta\theta}{\Delta\phi_i}\left[B_{i+1} - B_i + \frac{i(|B|_{i+1} - |B|_i)(e^{i\phi_{i+1}} - e^{i\phi_i})}{\Delta\phi_i}\right]$$

where $$\Delta\theta = \theta_{i+1} - \theta_i,\ B_{i+1} = B(\omega,\theta_{i+1}),\ |B_{i+1}| = |B(\omega,\theta_{i+1})|$$

and $$\Delta\phi_i = \phi(\theta_{i+1}) - \phi(\theta_i)$$

For intervals where $\Delta\phi_i = 0$, the above equation does not apply. Instead:

$$\Delta I_i = \int_{\theta_i}^{\theta_{i+1}} (a_i\theta + b_i)e^{in_i} d\theta = e^{i\phi_i}(|B|_{i+1} - |B|_i)\frac{\Delta\theta}{2}$$

The total integral is given by the sum of all increments,

$$I = \sum_{i=1}^{n-1} \Delta I_i$$

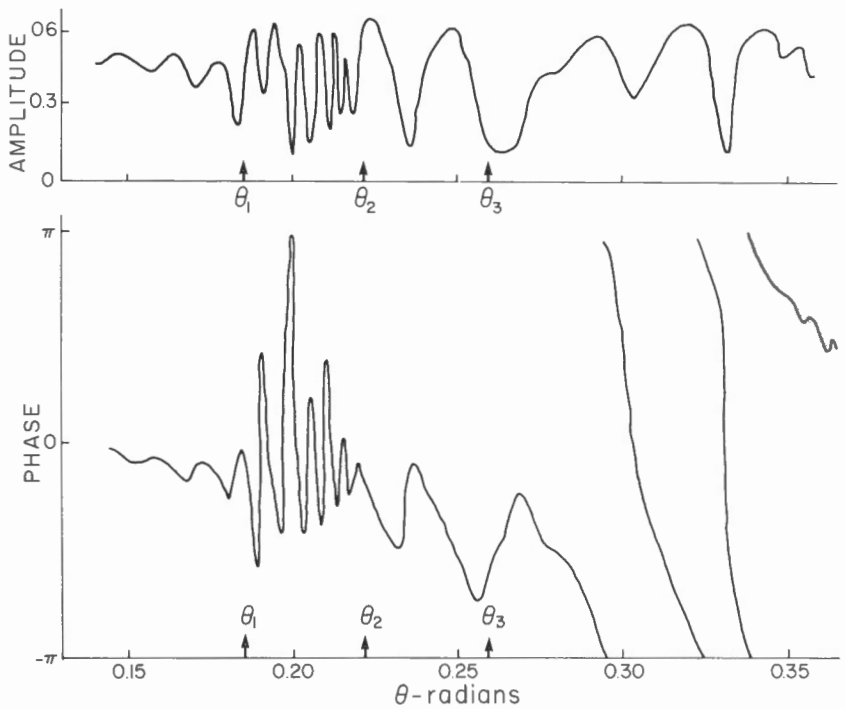

Figure 6. An example of the variation of amplitude and phase of the integrand over θ. These values correspond to model 1, given in Table 2. The angles, θ_1, θ_2, and θ_3 are critical angles of reflection at the upper surface of the 8.0, 6.8, and 5.9 km/s layers respectively.

Table 2

Test Model 1 — Oceanic Crust

M = 6, AO = 1.5, RO = 1.0, XH = 3.0

Layer No.	A(I)	B(I)	R(I)	D(I)	QP(I)	QS(I)	INDC(I)
1	1.8	0.80	1.50	0.0	100.0	50.0	0
2	2.0	1.20	2.00	0.005	100.0	50.0	0
3	4.5	2.61	2.70	0.5005	200.0	100.0	0
4	5.9	3.41	2.85	1.5005	300.0	150.0	0
5	6.8	3.93	3.00	2.005	500.0	300.0	0
6	8.0	4.62	3.30	6.005	600.0	450.0	0

NOTE: INDC(I) = 0 for all layers. Therefore the complete solution is calculated for V_{pp} and V_{ps}.

N	NW	NT	WO	DELF	PHIO	DELP	TI	DELT
400	155	100	3.28	0.1	5.0°	0.1°	-0.1	0.02

XR = 30, TO = 7.0

A complication arises in this numerical integration procedure because the quantity $\Delta\phi_i = \phi(\theta_{i+1})-\phi(\theta_i)$ is only known to $\pm 2n\pi$. Values of phase, $\phi(\theta)$, are formed from the equation

$$\phi(\theta) = \text{atan}[\text{ImB}(\omega,\theta)/\text{ReB}(\omega,\theta)]$$

and the arctangent is limited to the interval $-\pi$ to π, leading to discontinuities in the numerical values of ϕ for some values of θ and hence in $\Delta\phi$. This problem was overcome by making the reasonable assumption that, for small $\Delta\theta$, the true change in phase, $\Delta\phi$, is the minimum possible value. That is, $\Delta\phi = \min(\Delta\phi_c, \Delta\phi_c - 2\pi, \Delta\phi_c + 2\pi)$ where $\Delta\phi_c$ is the value calculated using the arctangent. These discontinuities in $\Delta\phi$ are illustrated in Figure 6 where unadjusted values of the phase of $B(\omega,\theta)$ are plotted.

This method of integration is rather crude. However, more elegant methods do not apply in this case where both the amplitude and phase of the integrand vary rapidly with θ (Davis and Rabinowitz, 1967). Furthermore, as the results show, the method is effective and sufficiently accurate to produce the desired seismograms. Figure 6 presents an example of the amplitude and phase variations of the function $B(\omega,\theta)$ and the corresponding model is given in Table 2.

The integration procedure is repeated for all frequencies at which the spectrum $S(\omega)$ is desired and at all source-receiver ranges, r, at which seismograms are to be obtained.

Numerical integration of the spectrum

The Fourier Transform of the spectrum, $S(\omega)$, is found by numerical integration to obtain the synthetic seismogram.

$$S(t) = \int_{-\infty}^{\infty} S(\omega)e^{-i\omega t}d\omega$$

The function $S(\omega)$ may be a rapidly varying function of ω. One of the reasons for this is that $S(\omega)$ contains an exponential term, $e^{i\omega t}A$, where t_A is the first arrival time. We are not interested in the synthetic seismogram before the first arriving energy and it is important to remove as much of the non-essential variations of the function $S(\omega)$ as possible. Therefore, before integration is carried out, the function $S(\omega)$ is premultiplied by the exponential, $e^{-i\omega t_0}$, where $t_0 \simeq t_A$. This effectively shifts the time origin from $t = 0$ to $t = t_0$ and the earliest energy will arrive shortly after t_0 if this quantity has been correctly chosen. The values of t_0, corresponding to a particular model for a seismogram at a given range, are presently part of the input to the program. However, they can be calculated by the program through the addition of a subroutine to determine first arrival times.

The numerical integration is performed in a similar way to the integration in the θ-plane. However, instead of approximating the amplitude and phase by straight lines in each interval, $\Delta\omega$, the real and imaginary parts of the function, $S(\omega)$, are approximated by straight lines. Use is also made of the fact that $s(t)$ is a real function so that

$$s(t) = \int_{-\infty}^{\infty} S(\omega)e^{-i\omega t}d\omega = 2\int_{0}^{\infty} \text{Re}[S(\omega)]\cos\omega t d\omega + 2\int_{0}^{\infty} \text{Im}[S(\omega)]\sin\omega t d\omega$$

Table 3

Computer Input Parameters

Card No.	Parameter	Description
1	N	The number of angles, r, at which V_{pp}, V_{ps} are evaluated.
	M	The number of layers in the model, including the lower half space but not the water layer.
	NW	The number of frequencies at which the spectrum is calculated.
	NR	The number of ranges, r, at which the synthetic seismograms are calculated.
	NT	The number of points, t, at which a synthetic seismogram is calculated.
	NL	The number of points (frequencies) at which the instrument response is given.
2	WO	The lowest angular frequency to be considered.
	DELF	The frequency increment – in hertz.
	PHIO	The minimum angle of incidence, θ_{min}, to be considered – in degrees.
	DELP	The increment in angle, $\Delta\theta$ – in degrees.
	T1	The minimum time at which the synthetic seismogram is to be evaluated. This time is to be given with respect to TO (see text) – in seconds.
	DELT	The time increment, Δt, giving the spacing between points at which the seismogram is calculated – in seconds.
	AO	The velocity in the upper medium (water) containing the source and receiver – in km/s.
	RO	The density in the upper medium – in g/cm^3.
	XH	The distance of the source from the first boundary (z_1-h) in kilometres.
	AR	The distance, a, from the source at which the pressure response due to an explosion is evaluated – usually taken at 10 m (see Section 1).
3	XR(K)	Horizontal source-receiver range in kilometres.
ONE CARD PER RANGE, NR CARDS TOTAL	WW(K)	Charge size for explosive at range XR(K) in pounds.
	DO(K)	Detonation depth below sea surface for explosive at range XR(K) in metres.
4	A(I)	P wave velocity in I^{th} layer – km/s.
ONE CARD PER LAYER, M CARDS TOTAL	B(I)	S wave velocity in I^{th} layer – km/s.
	R(I)	Density in I^{th} layer – g/cm^3.
	D(I)	Depth from sea floor to top of I^{th} layer – kilometres.
	QP(I)	Specific P wave attenuation factor for I^{th} layer.
	QS(I)	Specific S wave attenuation factor for I^{th} layer.
	INDC(I)	The q_{max} discussed in Section 5. INDC(I) therefore specifies the number of multiple reflections to be considered in the I^{th} layer. If INDC(I) = 0, the complete solution for the reflection coefficient is given.
5	FREQ(L)	The frequency in hertz at which the instrument response XB(L) is specified.
ONE CARD PER FREQUENCY, NL CARDS TOTAL	XB(L)	The instrument response represented as a complex number (not as amplitude and phase).

Table 4

Model Parameters after Fuchs (1968)

M = 7, AO = 6.40, RO = 3.00, XH = 59

Layer No.	A(I)	B(I)	R(I)	D(I)	QP(I)	QS(I)	INDC(I)
1	6.41	3.69	3.00	0.0	0.0	0.0	0
2	6.57	3.80	3.03	0.005	0.0	0.0	0
3	6.91	4.00	3.09	0.205	0.0	0.0	0
4	7.29	4.21	3.15	0.405	0.0	0.0	0
5	7.65	4.42	3.21	0.605	0.0	0.0	0
6	8.01	4.63	3.27	0.805	0.0	0.0	0
7	8.20	4.73	3.30	1.005	0.0	0.0	0

NOTE: The upper layer in this case, with a P velocity of 6.4 km/s, is obviously not water but must be a fluid. Since the model was used to compare calculated seismograms with those of Fuchs (1968) who considered only incident P waves the fact that the upper layer is fluid will make little difference to the results.

THE USE OF THE COMPUTER PROGRAM

Basic assumptions

The following assumptions have been made in the computations:

(a) The earth can be represented by a stack of flat-lying layers in each of which the P and S velocities and density can be specified. Velocity gradients within the structure can be approximated by many thin homogeneous layers.

(b) Surface waves and interface waves are not important either because the source or receiver is sufficiently far removed from the nearest boundary that they are not generated or observed, or because they are late-arriving signals which will not affect the part of the seismogram being considered.

(c) The source and receiver are sufficiently far apart that the Bessel functions, $J_0(kr\sin\theta)$ and $J_1(kr\sin\theta)$, can be represented by their asymptotic forms. This implies that $kr\sin\theta \gg 1$.

(d) The source and receiver are located in sea water, the receiver being located on the sea floor.

(e) The water layer is sufficiently thick that multiple reflections within this layer are unimportant. They are arrivals appearing later in time than the arrivals being considered.

(f) The source function may be represented by an explosive charge, including the shock wave, first and second bubble pulses, and associated surface reflections. The charge size and detonation depth are known.

(g) The instrument response is known.

(h) The vertical particle velocity is desired.

Of these assumptions, the first three are most binding. With little additional effort the computer program could be modified to include a solid surface layer and different source functions other than those for explosives. The positions of the source and receiver could be changed, to the free surface of a solid, for example. The instrument response must be known if the true waveforms are to be reproduced. However, if the approximate frequency bandwidth of the instruments or of the combined source and instrument response is known, useful comparsions of relative signal amplitudes as functions of distance and time for observed and synthetic seismograms can be made (Fuchs and Muller, 1971; Fowler, 1976).

Input parameters

The computer program is written in FORTRAN IV for a CDC 7600 computer. The input is punched on cards and the output is written on a line printer. The input parameters are listed and described in order of card input in Table 3.

An example is perhaps the best way of illustrating the determination of these parameters. The model used approximates the standard oceanic crustal structure and model parameters are listed in Table 2. As previously noted, Figure 6 shows the behavior of the integrand as a function of θ for the same model. The oscillations in amplitude and phase suggest that very small increments in $\Delta\theta$ must be taken in order to obtain an accurate estimation of the integral over θ. The oscillations are most rapid between $\theta = \theta_1$ and θ_2 (Fig. 6). Physically this corresponds to angles of incidence greater than the critical angle for P reflection at the lowest interface (Moho) and less than the critical angle for P reflection at the interface between the 5.9 and 6.8 km/s layers. That is, the oscillations shown in Figure 6 between θ_1 and θ_2 are due to multiple reverberations within the 6.8 km/s layer. For angles greater than θ_2 these oscillations are less rapid and this is caused primarily by the decrease in layer thickness and consequent decrease in travel time through the structure for angles greater than θ_2, the critical angle for P reflection at the top of the 6.8 km/s layer. In general, a good guideline for selecting the correct increment in angle, $\Delta\theta$, is

$$2fh_i \left(\frac{\frac{\alpha_i}{\alpha_{i+1}\alpha_0}\sqrt{1 - \frac{\alpha_0^2}{\alpha_{i+1}^2}}}{\sqrt{1 - \frac{\alpha_i^2}{\alpha_{i+1}^2}}} \right) \Delta\theta \ll 1$$

where h_i is the thickness of any layer in the model, α_i, α_{i+1} and α_0 and P wave velocities (or S wave velocities) and f is the frequency. Relating this to test model 1 for the 6.8 km/s layer, $\Delta\theta = 0.0017$ rad and, therefore, $0.14 \ll 1$. Note that the above relation states that the increment in θ will be much less than the period at which the oscillations are occurring in the integrand (Fig. 6).

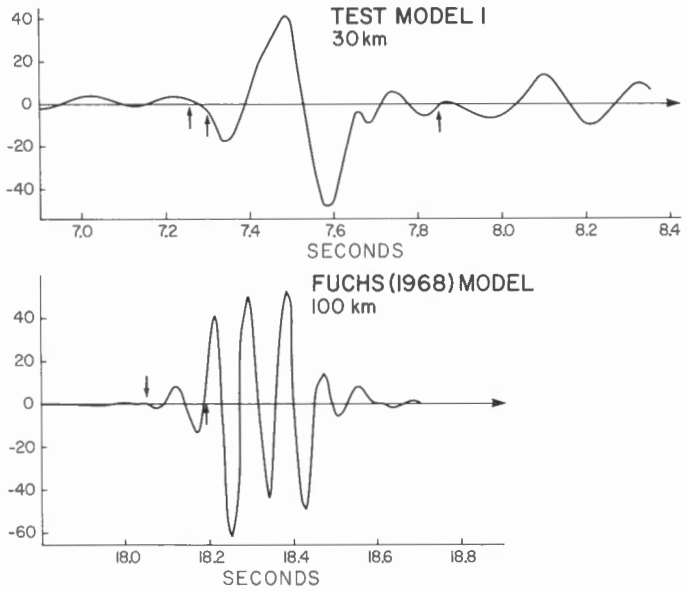

Figure 7. Synthetic seismograms corresponding to the models given in Tables 2 and 4, and described in the text. The arrows denote the arrival times for particular ray paths through the models.

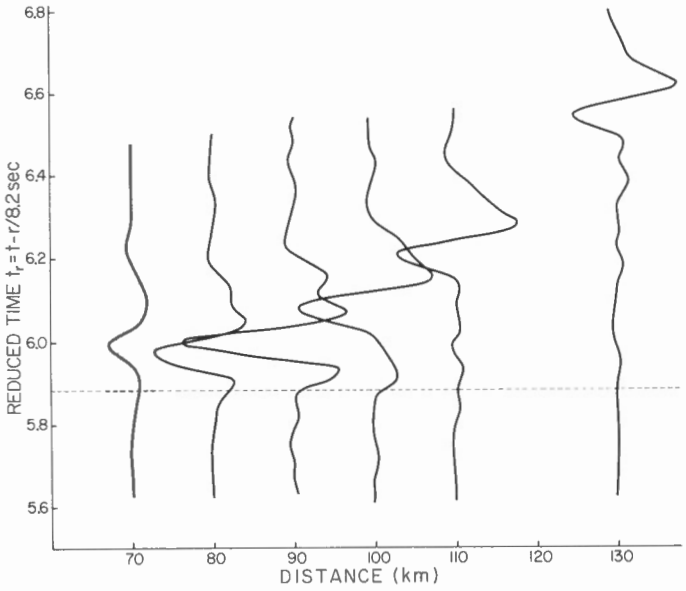

Figure 8. Synthetic seismograms corresponding to the model given in Table 4. These are presented using a reduced travel time, calculated for a 8.2 km/s velocity. The dashed line indicates the arrival time of the mantle head wave. This figure can be directly compared to the equivalent diagram presented by Fuchs (1968, his Fig. 8).

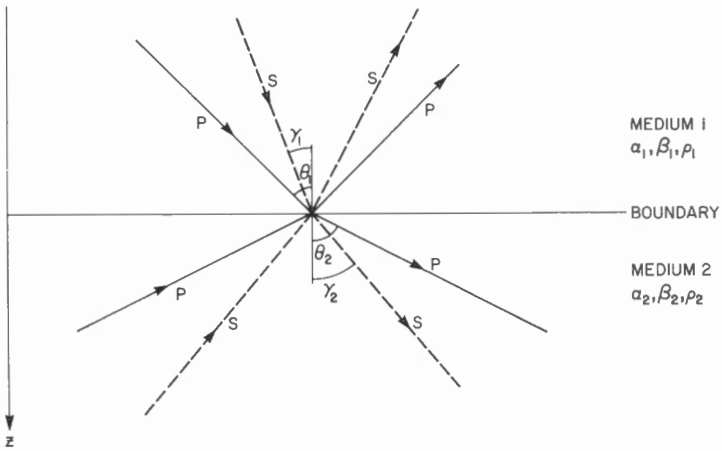

Figure 9

Plane waves incident and reflected at a boundary between two elastic media. All possible P and S propagation paths are shown. S waves paths are dashed lines; P waves are solid lines.

The range of integration in θ is fixed by θ_{min} = PHIO and θ_{max} = PHIO + N · DELP. These angles correspond to apparent velocities of 17.2 and 2.1 km/s which span the range of desired apparent velocities. Most early arriving energy at a range of 30 km for model 1 will come from the refracted and reflected P wave arrivals from the mantle and lower crust, with apparent velocities between about 10 km/s and 6.8 km/s. The range of apparent velocities used includes probable values for apparent S velocities from these layers also.

The parameters, NW, DELF and WO are dictated by the frequency bandwidth of the recorded signals and the size of the interval, $\Delta\omega$, necessary to use the trapezoidal rule for numerical integration of the spectrum. The bandwidth used in model 1 was centred at 5 Hz and extended from 0.5 to 15 Hz. The effects of an explosive source were not considered in these calculations. The frequency increment $\Delta\omega$ must be chosen so that, if significant energy is observed over time interval t, $t\Delta\omega << 2\pi$ or $t\Delta f << 1$. The example included as input T1 = -0.1 and TO = 7. This means that the program will begin to calculate the synthetic seismogram at an actual time of 6.90 s after the explosion, while the first arrival time in this case is 7.25 s at 30 km range.

Computer times in the CDC 7600 are 300 s for N = 400, NW = 310, NR = 4 and M = 7. By far the largest proportion of time is spent calculating the coefficients $Vpp(\omega,\theta)$ and $Vps(\omega,\theta)$. Relatively little is spent in the numerical integration and increasing NR or NT are therefore insignificant in terms of computation time.

Some examples of synthetic seismograms

Figure 7 shows the synthetic seismogram corresponding to model 1. The first arrival for this range is the P wave refracted along the top of the 6.8 km/s layer, closely followed by the P wave refracted along the top of the 8.0 km/s layer. These two events occur within 0.04 s and cannot be separated. They are followed closely by their associated reflections. The other large event centred at 8.1 s is probably related to reflection and refraction along the top of the 5.8 km/s layer. There is some noise evident before the first arrival in this example which could be eliminated by using a finer grid in $\Delta\theta$ and $\Delta\omega$. The user must decide between computer time expense and accuracy according to his needs.

The second example shown in Figure 7 was obtained for a simple model of one interface between two half spaces in which the interface is a linear velocity gradient 1 km thick (Table 4). The model is the same as that presented by Fuchs (1968, his Fig. 8) and was used to test the program by comparing the synthetic seismograms for similar source-receiver bandwidths to those obtained by him. The seismogram in Figure 7 was calculated using an explosive source of 90 kg at a depth of 100 m below the upper surface and the instrument response shown in Figure 5. The arrival times of the refracted and reflected P waves are indicated and it is interesting to note that the reflected wave is about six times greater in amplitude than the refracted wave. Similar relationships have been noted by many authors (Cerveny and Ravindra, 1971).

Finally, in Figure 8, a set of synthetic seismograms corresponding exactly to those presented by Fuchs (1968, his Fig. 8) is shown. Those calculated using the computer program given here closely match those presented by Fuchs, providing confidence in the computational methods offered in this paper.

REFERENCES

Barrett, D.L., Heffler, D.E., and Keen, C.E.
1977: Ocean bottom seismometer developments; in Report of Activities, Part B, Geol. Surv. Can., Paper 77-1B, p. 129-132.

Brekhovskikh, L.M.
1960: Waves in layered media; Academic Press, New York.

Cerveny, V. and Ravindra, R.
1971: Theory of seismic head waves; University of Toronto Press, Toronto.

Davis, P.J. and Rabinowitz, P.
1967: Numerical integration; Blaisdell, Toronto.

Ewing, W.M., Jardetsky, W.S., and Press, F.
1957: Elastic waves in layered media; McGraw-Hill, New York.

Fowler, C.M.R.
1976: Crustal structure of the Mid-Atlantic Ridge crest at 37°N; Geophys. J., v. 47, p. 459-491.

Fuchs, K.
1968: The reflection of spherical waves from transition zones with arbitrary depth-dependent elastic moduli and density; J. Physics Earth, v. 16, special issue 27.

Fuchs, K. and Muller, G.
1971: Computation of synthetic seismograms with the reflectivity method and comparisons with observations; Geophys. J., v. 23, p. 417-433.

Heelan, P.A.
1953: On the theory of head waves; Geophysics, v. 18, p. 871-893.

Hyndman, R.D., Roders, G.C., Bone, M.N., Lister, C.R.B., Wade, U.S., Barrett, D.L., Davis, E.E., Lewis, T., Lynch, S., and Seemann, D.
Geophysical measurements in the region of the Explorer Ridge off Western Canada; Can. J. Earth Sci. (in press).

Keen, C.E.
1977: Report of Cruise 77-014; Bedford Institute of Oceanography.

Kennett, B.L.N.
1974: Reflections, rays, and reverberations; Seismol. Soc. Am., Bull., v. 64, p. 1685-1696.

1975: The effects of attenuation on seismograms; Seismol. Soc. Am., Bull., v. 65, p. 1643-1651.

1977: Towards a more detailed seismic picture of the oceanic crust and mantle; Mar. Geophys. Res., v. 8, p. 7-42.

Knopoff, L.
1964: Q; Rev. Geophys., v. 2, p. 625-660.

Lewis, B.T.R. and Syndsman, W.E.
1977: Evidence for a low-velocity zone at the base of the oceanic crust; Nature, v. 266, p. 340-344.

Orcutt, J.A., Kennett, B.L.N., and Dorman, L.M.
1976: Structure of the East Pacific Rise from an ocean bottom seismometer survey; Geophys. J., v. 45, p. 305-320.

Phinney, R.A.
1961: Leaking modes in the crustal waveguide, 1, The oceanic PL wave; J. Geophys. Res., v. 66, p. 1445-1452.

Weston, D.E.
1960: Underwater explosions as acoustic sources; Physical Soc. Lond., Proc., v. 76, p. 233-249.

Young, G.B. and Braille, L.W.
1976: A computer program for the application of Zoeppritz's amplitude equations and Knott's energy equations; Seismol. Soc. Am., Bull., v. 66, p. 1881-1885.

APPENDIX 1

List of Symbols

α,β,ρ	P wave and S wave velocities and density in an elastic body
f	frequency in hertz
h	depth of the source below sea surface
J_0,J_1	Bessel functions of order 0 and 1 respectively
k	wave number, $k = \omega/v$ where v is the velocity (P or S) in an elastic body
p	acoustic pressure
Q	quality factor, or specific attenuation factor for P or S propagation through an elastic body
r_{ij}^{D}, r_{ij}^{U}	plane wave reflection coefficients for reflection of an incident wave from above or below an interface between two elastic solids. The indices i,j can refer to P or S propagation; i indicates the nature of the incident wave, and j the nature of the reflected wave. Hence r_{ps}^{U} indicates the coefficient for reflection of a wave incident as a P wave in the lower solid and reflected as an S wave
t_{ij}^{D}, t_{ij}^{U}	plane wave transmission coefficients with the same superscripts and subscripts as for the reflection coefficients. Thus t_{ss}^{D} indicates the transmission coefficient for a shear wave incident from the upper solid through the boundary and propagating as a shear wave in the lower solid
ϕ	compressional wave displacement potential
ψ	shear wave displacement potential
θ	angle of incidence of a plane wave. Usually with reference to incidence from the water onto the sea floor
r	horizontal range from source to receiver
t	time (in seconds)
u_x,u_z	components of particle displacement in Cartesian
u_r,u_z	or cylindrical co-ordinates
$V_{pp}(\omega,\theta)$	the generalized plane wave reflection coefficient for incident P/reflected P waves
$V_{ps}(\omega,\theta)$	the generalized plane wave reflection coefficient for incident P/reflected S
ω	angular frequency
z	depth measured positive downward, z = 0 is the sea floor

APPENDIX 2

Plane Wave Reflection and Transmission Coefficients

A. Simple Plane Wave Coefficients from a Single Interface

At a single plane interface separating two elastic solids, the boundary conditions, continuity of particle displacement u_x and u_z and of the stresses tangential and perpendicular to the boundary, τ and σ respectively, are used to obtain the reflection and transmission coefficients. This procedure has been described often in the literature [see Young and Braille (1977) for a list of references]; however, it is worth repeating here because, as Young and Braille (1977) have noted, there are many errors in the published results.

The plane waves travelling in the upper solid (medium 1, Fig. 8) are represented as their P and S wave displacement potentials;

$$\phi_1 = A_1 e^{ik_1 x\sin\theta_1 + ik_1 z\cos\theta_1} + A_2 e^{ik_1 x\sin\theta_1 - ik_1 z\cos\theta_1}$$

$$\psi_1 = B_1 e^{ik_1 x\sin\theta_1 + ik_1' z\cos\gamma_1} + B_2 e^{ik_1 x\sin\theta_1 - ik_1' z\cos\gamma_1}$$

where k_1' is the wave number for S wave propagation in the upper medium and γ_1 is the angle of incidence of an S wave on the boundary (Fig. 9).

In the lower medium the wave potentials are:

$$\phi_2 = C_1 e^{ik_2 x\sin\theta_2 + ik_2 z\cos\theta_2} + C_2 e^{ik_2 x\sin\theta_2 - ik_2 z\cos\theta_2}$$

$$\psi_2 = D_1 e^{ik_2 x\sin\theta_2 + ik_2' z\cos\gamma_2} + D_2 e^{ik_2 x\sin\theta_2 - ik_2' z\cos\gamma_2}$$

In each of the above four equations the first term represents a wave propagating down, in the positive z direction, and the second term represents a wave propagating in the negative z direction. The displacements and stresses are related to these wave potentials by the equations

$$u_z = \frac{\partial\phi}{\partial z} + \frac{\partial\psi}{\partial x}, \quad u_x = \frac{\partial\phi}{\partial x} - \frac{\partial\psi}{\partial z}, \quad \tau = \mu\left(\frac{2\partial^2\phi}{\partial x\partial z} + \frac{\partial^2\psi}{\partial x^2} - \frac{\partial^2\psi}{\partial z^2}\right)$$

$$\sigma = \lambda\nabla^2\phi + 2\mu\left(\frac{\partial^2\phi}{\partial z^2} + \frac{\partial^2\psi}{\partial x\partial z}\right)$$

The wave potentials in the upper and lower media are differentiated to obtain the displacements and stresses and equate these quantities derived for the upper and lower media at the boundary. The boundary is considered coincident with the level z = 0. These steps give the following four equations:

$$2\rho_1\sin^2\gamma_1\frac{\cos\theta_1}{\sin\theta_1}(A_1-A_2) - \rho_1(\cos^2\gamma_1-\sin^2\gamma_1)(B_1+B_2)$$

$$= 2\rho_2\sin^2\gamma_2\frac{\cos\theta_2}{\sin\theta_2}(C_1-C_2) - \rho_2(\cos^2\gamma_2-\sin^2\gamma_2)(D_1+D_2)$$

$$\rho_1(\cos^2\gamma_1-\sin^2\gamma_1)(A_1+A_2) + 2\rho_1\sin\gamma_1\cos\gamma_1(B_1+B_2)$$

$$= \rho_2(\cos^2\gamma_2-\sin^2\gamma_2)(C_1+C_2) + 2\rho_2\sin\gamma_2\cos\gamma_2(D_1-D_2)$$

$$(A_1+A_2) - \frac{\cos\gamma_1}{\sin\gamma_1}(B_1-B_2) = (C_1+C_2) - \frac{\cos\gamma_2}{\sin\gamma_2}(D_1-D_2)$$

$$\frac{\cos\theta_1}{\sin\theta_1}(A_1-A_2) + (B_1+B_2) = \frac{\cos\theta_2}{\sin\theta_2}(C_1-C_2) + (D_1+D_2)$$

These four equations yield four unknowns. For example, a P wave incident from the first medium onto the boundary gives the amplitude coefficients related to the following waves:

A_1 = incident P, A_2 = reflected P, B_1 = 0 (incident SV),

B_2 = reflected SV, C_1 = transmitted P, D_1 = refracted SV,

$C_2 = D_2 = 0$ (no reflected waves in the lower medium).

These four unknowns may be found from the four equations either in explicit terms (Young and Braille, 1977) or by solving the corresponding matrix equations. Furthermore, the reflection and transmission coefficients associated with an S wave, incident from the first medium, and with P and S waves incident from the second medium, can be similarly found, giving the 16 reflection and transmission coefficients for the boundary.

I have used the explicit form of the equations for the reflection and transmission coefficients (Young and Braille, 1977; Cerveny and Ravindra, 1971). However, for completeness, I present the matrix formulation below. All coefficients discussed here are displacement potential coefficients [Type II of Young and Braille (1977)].

In matrix form the equations are:

$$E^D \cdot \begin{pmatrix} r_{pp}^D \\ r_{ps}^D \\ t_{pp}^D \\ t_{ps}^D \end{pmatrix} = \begin{pmatrix} -2\rho_1 \sin^2\gamma_1 \cos\theta_1/\sin\theta_1 \\ -\rho_1(\cos^2\gamma_1 - \sin^2\gamma_1) \\ -1 \\ -\cos\theta_1/\sin\theta_1 \end{pmatrix} \qquad E^u \cdot \begin{pmatrix} r_{pp}^u \\ r_{ps}^u \\ t_{pp}^u \\ t_{ps}^u \end{pmatrix} = \begin{pmatrix} 2\rho_2 \sin^2\gamma_2 \cos\theta_2/\sin\theta_2 \\ -\rho_2(\cos^2\gamma_2 - \sin^2\gamma_2) \\ -1 \\ \cos\theta_2/\sin\theta_2 \end{pmatrix}$$

$$E^D \cdot \begin{pmatrix} r_{sp}^D \\ r_{ss}^D \\ t_{sp}^D \\ t_{ss}^D \end{pmatrix} = \begin{pmatrix} \rho_1(\cos^2\gamma_1 - \sin^2\gamma_1) \\ -2\rho_1 \sin\gamma_1 \cos\gamma_1 \\ \cos\gamma_1/\sin\gamma_1 \\ -1 \end{pmatrix} \qquad E^u \cdot \begin{pmatrix} r_{sp}^u \\ r_{ss}^u \\ t_{sp}^u \\ t_{ss}^u \end{pmatrix} = \begin{pmatrix} \rho_2(\cos^2\gamma_2 - \sin^2\gamma_2) \\ 2\rho_2 \sin\gamma_2 \cos\gamma_2 \\ -\cos\gamma_2/\sin\gamma_2 \\ -1 \end{pmatrix}$$

where E^D, E^u are 4x4 matrices and may have complex elements.

$$E_{11}^D = -2\rho_1 \sin^2\gamma_1 \frac{\cos\theta_1}{\sin\theta_1} \qquad E_{11}^u = 2\rho_2 \sin^2\gamma_2 \frac{\cos\theta_2}{\sin\theta_2}$$

$$E_{12}^D = -\rho_1(\cos^2\gamma_1 - \sin^2\gamma_1) \qquad E_{12}^u = -\rho_2(\cos^2\gamma_2 - \sin^2\gamma_2)$$

$$E_{13}^D = -2\rho_2 \sin^2\gamma_2 \frac{\cos\theta_2}{\sin\theta_2} \qquad E_{13}^u = 2\rho_1 \sin^2\gamma_1 \frac{\cos\theta_1}{\sin\theta_1}$$

$$E_{14}^D = \rho_2(\cos^2\gamma_2 - \sin^2\gamma_2) \qquad E_{14}^u = \rho_1(\cos^2\gamma_1 - \sin^2\gamma_1)$$

$$E_{21}^D = \rho_1(\cos^2\gamma_1 - \sin^2\gamma_1) \qquad E_{21}^u = \rho_2(\cos^2\gamma_2 - \sin^2\gamma_2)$$

$$E_{22}^D = -2\rho_1 \sin\gamma_1 \cos\gamma_1 \qquad E_{22}^u = 2\rho_2 \sin\gamma_2 \cos\gamma_2$$

$$E_{23}^D = -\rho_2(\cos^2\gamma_2 - \sin^2\gamma_2) \qquad E_{23}^u = -\rho_1(\cos^2\gamma_1 - \sin^2\gamma_1)$$

$$E_{24}^D = -2\rho_2 \sin\gamma_2 \cos\gamma_2 \qquad E_{24}^u = 2\rho_1 \sin\gamma_1 \cos\gamma_1$$

$$E_{31}^D = 1 \qquad E_{31}^u = 1$$

$$E_{32}^D = \cos\gamma_1/\sin\gamma_1 \qquad E_{32}^u = -\cos\gamma_2/\sin\gamma_2$$

$$E_{33}^D = -1 \qquad E_{33}^u = -1$$

$$E_{34}^D = \cos\gamma_2/\sin\gamma_2 \qquad E_{34}^u = -\cos\gamma_1/\sin\gamma_1$$

$$E_{41}^{D} = -\cos\theta_1/\sin\theta_1 \qquad E_{41}^{u} = \cos\theta_2/\sin\theta_2$$

$$E_{42}^{D} = 1 \qquad E_{42}^{u} = 1$$

$$E_{43}^{D} = -\cos\theta_2/\sin\theta_2 \qquad E_{43}^{u} = \cos\theta_1/\sin\theta_1$$

$$E_{44}^{D} = -1 \qquad E_{44}^{u} = -1$$

The reflection and transmission coefficients are complicated functions of the angles of incidence. If given the angle of incidence, θ_1 or γ_1, for example, the angle of propagation in the other media, γ_2 and θ_2 must be found. Using Snell's Law, when a P wave is incident from medium 1,

$$\cos\theta_2 = \pm\sqrt{1 - \frac{\alpha_2^2}{\alpha_1^2}\sin^2\theta_1}$$

$$\cos\gamma_1 = \pm\sqrt{1 - \frac{\beta_2^2}{\alpha_1^2}\sin^2\theta_1}$$

and the appropriate sign of the square root must be chosen. These quantities become imaginary (or complex for complex P and S velocities) when $(\alpha_2)/(\alpha_1)\sin\theta_1 > 1$ or $(\beta_2)/(\alpha_1)\sin\theta_1 > 1$. In this case the sign of the square root must be selected such that Im $\cos\theta_2$ and Im $\cos\gamma_2$ are positive. Only then will the plane wave propagation decrease exponentially with increasing z when the angle for critical reflection is exceeded.

B. Phase Related Reflection Coefficients

Calculation of the simple plane wave reflection and transmission coefficients involves the restriction that the boundary coincides with z = 0. This cannot be true for all interfaces in a stack of layers such as in the models considered here. In this case, the reflection coefficients for any boundary are calculated as described in part A but the boundary now lies at an arbitrary depth z = h and exponential propagation terms will appear in the coefficients. When this is done, Kennett's (1974) equations for the phase-related reflection coefficients become,

$$R_D = \begin{vmatrix} r_{pp}^{D} e^{2ik_1 h\cos\theta_i} & r_{sp}^{D} e^{ik_1 h\cos\gamma_1 + ik_1 h\cos\theta_1} \\ r_{ps}^{D} e^{ik_1' h\cos\gamma_1 + ik_1 h\cos\theta_1} & r_{ss}^{D} e^{2ik_1' h\cos\gamma_i} \end{vmatrix}$$

$$R_U = \begin{vmatrix} r_{pp}^{u} e^{-2ik_2 h\cos\theta_2} & r_{sp}^{u} e^{-ik_2' h\cos\gamma_2 - ik_2 h\cos\theta_2} \\ r_{ps}^{u} e^{-ik_2 h\cos\theta_2 - ik_2' h\cos\gamma_2} & r_{ss}^{u} e^{-2ik_2' h\cos\gamma_2} \end{vmatrix}$$

$$T_D = \begin{vmatrix} t_{pp}^{D} e^{ik_1 h\cos\theta_1 - ik_2 h\cos\theta_1} & t_{sp}^{D} e^{ik_1' h\cos\gamma_1 - ik_2 h\cos\theta_2} \\ t_{ps}^{D} e^{ik_1 h\cos\theta_1 - ik_2' h\cos\gamma_2} & t_{ss}^{D} e^{ik_1' h\cos\gamma_1 - ik_2' h\cos\gamma_2} \end{vmatrix}$$

$$T_u = \begin{vmatrix} t_{pp}^{u} e^{ik_1 h\cos\theta_1 - ik_2 h\cos\theta_2} & t_{sp}^{u} e^{ik_1 h\cos\theta_1 - ik_2' h\cos\gamma_2} \\ t_{ps}^{u} e^{ik_1' h\cos\gamma_1 - ik_2 h\cos\theta_2} & t_{ss}^{u} e^{ik_1' h\cos\gamma_1 - ik_2' h\cos\gamma_2} \end{vmatrix}$$

In these equations r_{pp}^{D}, r_{ss}^{u}, t_{ps}^{D}, etc., are the simple reflection and transmission coefficients with no phase term. The subscripts 1 and 2 could be replaced by the subscripts i and i+1, for the i+1 boundary within the stack of layers.

Numerical difficulties present themselves when the exponential phase terms are calculated if one or more of the cosines become imaginary (the corresponding critical angle is exceeded). Then, the matrices R_u, T_D, and T_u will contain large positive, real exponential elements which can lead to significant roundoff errors in the calculations. These large exponential terms represent plane wave propagation paths which are not physically realistic because the angle of critical reflection has been exceeded. This justified the omission of elements in the above matrices when their exponents exceed a certain value. When the absolute value of the exponent,

$$\left| \frac{\omega d_i}{V_i} \sqrt{\frac{V_i^2 \sin^2\theta - 1}{\alpha_0^2}} \right|$$

is greater than 20, the computer program sets the corresponding matrix element equal to zero. Here V_i is the P or S velocity in the i^{th} layer and d_i is its thickness. When all critical angles for propagation below an interface have been exceeded by the amount given above, the program ignores layers below it because there are no real propagation paths through this part of the layered structure.

APPENDIX 3

The Computer Program

The computer program is listed here, with comments concerning the function of various parts of the program. The main program controls the input and output, calls subroutines which calculate the generalized plane wave reflection coefficients and the source response. The main program also performs the numerical integration. The subroutine REFLECT calculates the generalized plane wave reflection coefficients using Kennett's (1974) method. It, in turn, calls subroutines RPLV which calculates the 16 reflection coefficients associated with one boundary and PHASE which sets up the four 2x2 matrices of phase-related reflection coefficients. In addition, inversion and multiplication of 2x2 complex matrices are performed in subroutines INVR and MULTC respectively. Subroutine SPLAT calculates the frequency response of an explosive source.

```
MSFORTRAN    (4.3) / MSOS 5.1                          16/12/77

      PROGRAM CK(INPUT=300,TAPE1=INPUT,OUTPUT)
      DIMENSION A(25),B(25),R(25),D(25),QP(25),QS(25),XR(10)
      DIMENSION FREQ(150),INDC(25),DO(10),WW(10)
      DIMENSION RPP(2000),RPS(2000),RPP1(2000),RPS1(2000),W(2000)
      COMPLEX BB(150),XI,P,PP
      COMPLEX XB(150)
      COMPLEX XJ
      COMPLEX SPEC(10,2000)
      COMMON RPP,RPS,RPP1,RPS1,W,SPEC
      LEVEL 2,RPP,RPS,RPP1,RPS1,W,SPEC
C
C
C     PROGRAM TO COLCULATE SYNTHETIC SEISMOGRAMS AT  RANGES XR AND  WATER
C     DEPTH XH. THIS VERSION GIVES VERTICALCOMPONENT  FOR  OBS.
C   PLANE HAVE REFL COEFFS CALCULATED IN REFLCT USING KENNETT 1974 BSSA
C     INDC INDICATES WHEN TO TRUNCATE HIS SERIES FOR MAULTIPLES
C     INDC=0 NO TRUNCATION N=NO OF ANGLES,PHIO=STARTING ANGLE IN DEGREES
C     DELP=INCREMENT  IN DEGREES,A0=WATER DEPTH,RO=WATER DENSITY,TO=TIME REMOVED
C     BY PREMULTIPLYING SPECTRA  BY EXP(IW*TO)
C     T1=STARTING TIME OF TIME SERIES,DELT=TIME INCREMENT,WO=START, FREQ
C     IN RADIANS,DELF FREQ INCRE. IN HZ,M=NO OF LAYERS,NW=NO OF FREQS,NT=NO OF T
C     TIMES,A=LAYER P VEL,B=LAYER S VEL,R=LAYER RHO,D=LAYER THICKNESS
C     QP=0 FOR VP,QS=0 FOR VS
C     XB(L)= INSTRU RESPONSE
C     BB(L)=SOURCE TIMES INSTRU RESPOMSE AT FREW =FREQ(L) L=1,NL
C     BB NEEDNT BE EQUISPACED NOR AT SAME FREQS AS CALCULATED
C     EARTH RESPONSE ONLY NEED TO BE CLOSE ENOUGH FOR LINEAR INTERP
C
C     INTEGRATION IN ANGLE AND FREQ DOMAINS BY APPROX PHASE ANGLE AND AMPLITUDE
C     BY STRAIGHT LINE  SEGMENTS IN DELP OR DELF. TO FIND PHASE ANGLE
C     USE ATAN2 THUS HAVE TO CHECK THAT IN CORRECT TUPI RANGE ONLY IMPORTANT
C    IN FINDING PHI(I+1)-PHI(I) IF ONE OR OTHER TERM IS OUT BY TUPI
C     USE MINIMUM OF THIS DIFFERENCRGE SO SHOULD BE SMOOTHLY VARYING
C
C     AR=RANGE IN M FOR SOURCE CALCS, WW=CHARGE SIZE IN LBS,DO=DETONATION
C     DEPTH IN M
C
C
C
      READ(1,101) N,M,NW,NR,NT,NL
      READ (1,102) WO,DELF,PHIO,DELP,T1,TO,DELT,AO,RO,XH,AR
      READ (1,105) (XR(K),WW(K),DO(K),K=1,NR)
      PRINT 206
      PRINT 205,(XR(K),WW(K),DO(K),K=1,NR)
      XI=CMPLX(0.,1.)
      TUPI=2.*3.1415926
      XJ=CEXP(-XI*TUPI/4.)
      PHI=0.017545*PHIO
      DELP=0.017545*DELP
      W(1)=WO
      DELF=DELF*TUPI
      DO 1 K=1,NR
      SPEC(K,1)=0.
      DO 1 J=2,NW
      SPEC(K,J)=0.
    1 W(J)=W(J-1)+DELF
```

Appendix 3 (cont'd)

```
      PRINT 200
      PRINT 201, N,M,NW,NR,NT,W0,DELF,PHI0,DELP,T1,DELT,A0,R0
      PRINT 202
      READ (1,100) (A(I),B(I),R(I),D(I),QP(I),QS(I),INDC(I),I=1,M)
      PRINT 203, (A(I),B(I),R(I),D(I),QP(I),QS(I),INDC(I),I=1,M)
      READ (1,103) (FREQ(L),XB(L),L=1,NL)
      NN=N-1
C     CALCULATE (NW=NO OF FREQS) PHASE RELATED REFL COEFFS OT PHI AND
C     PHI1
C     IN SAME PHI DO LOOP INTEGRATE BY ADDING INCREMENT IN PHI1-PHI
C     REFLCT RETURNS COEFFS FOR ARRAY
C     OF W RPP=ANP,RPS=PHASE
      I=1
      CS=COS(PHI)
      SS=SIN(PHI)
      CALL REFLCT(A,B,R,D,PHI,W,RPP,RPS,QP,QS,M,NW,A0,R0,INDC)
   22 PHI1=PHI+DELP
      CS1=COS(PHI1)
      SS1=SIN(PHI1)
      CALL REFLCT(A,B,R,D,PHI1,W,RPP1,RPS1,QP,QS,M,NW,A0,R0,INDC)
      DO 10 J=1,NW
      XK=W(J)/A0
      DP=RPS1(J)-RPS(J)
      DPPTU=DP+TUPI
      DPMTU=DP-TUPI
      DP1=AMIN1(ABS(DP),ABS(DPPTU),ABS(DPMTU))
      IF(DP1.EQ.ABS(DP)) GO TO 20
      IF(DP1.EQ.ABS(DPPTU)) DP=DPPTU
      IF(DP1.EQ.ABS(DPMTU)) DP=DPMTU
   20 XHXKCS=XH*XK*CS
      XHXKCS1=XH*XK*CS1
      XKSS1=XK*SS1
      XKSS=XK*SS
      RPPJ=RPP(J)
      RPP1J=RPP1(J)
      DP2=DP
      DO 14 K=1,NR
      PH1=XHXKCS1+XR(K)*XKSS1
      PH=XHXKCS+XR(K)*XKSS
      PP=CEXP(XI*(PH1+RPS1(J)))
      P=CEXP(XI*(PH+RPS(J)))
      DP=DP2+PH1-PH
      IF (DP.EQ.0.) GO TO 15
      SPEC(K,J)=SPEC(K,J)-XI*(RPP1J*PP-RPPJ*P+XI*(RPP1J-RPPJ)*(PP-P)/D
     1P)*DELP/DP
      GO TO 14
   15 SPEC(K,J)=SPEC(K,J)+P*(RPP1J+RPPJ)*DELP/2.
   14 CONTINUE
      RPP(J)=RPP1J
      RPS(J)=RPS1(J)
   10 CONTINUE
   23 PHI=PHI1
      SS=SS1
      CS=CS1
      I=I+1
      IF(I.NE.NN) GO TO 22
      DO 3 K=1,NR
      PRINT 204, T0
      DO 4 J=1,NW
      SPEC(K,J)=-SPEC(K,J)*CEXP(-XI*W(J)*T0)/(SQRT(XR(K)*TUPI))
      SPEC(K,J)=SPEC(K,J)*XJ*((W(J)/A0)**(3./2.))
    4 PRINT 204, W(J),SPEC(K,J)
C
C     CALCULATION OF SOURCE RESP AND TOTAL INST AND SOURCE RESP
C     INCLUDES SHOCH TWO BUBBLES AND SURFACE REFLECTION
      CALL SPLAT(WW(K),DO(K),BB,XB,FREQ,NL,AR)
C
```

Appendix 3 (cont'd)

```
C     INTEGRATION OF SPECTRUM USING MODIFIED TRAPEZOIDAL RULE FIRST WITH
C     MULTIPLY SOURCE INST RESP BY EARTH RESP INTERPOLATE IN BB(L)
      DO 12 J=1,NW
      FR=W(J)/TUPI
      DO 44 L=1,NL
      IF (FREQ(L)-FR) 44,77,88
   44 CONTINUE
   77 SPEC(K,J)=SPEC(K,J)*BB(L)
      GO TO 12
   88 SPEC(K,J)=SPEC(K,J)*(BB(L-1)+(BB(L)-BB(L-1))*(FR-FREQ(L-1)))/(FR
     1EQ(L)-FREQ(L-1))
   12 CONTINUE
C     FOURIER TRANSFORM
C
      NJ=NW-1
      TIME=T1
      DO 9 I=1,NT
      FT=0.
      TIME=TIME+DELT
      DO 17 J=1,NJ
      FT=FT+REAL(SPEC(K,J+1)-SPEC(K,J))*(COS(W(J+1)*TIME)-COS(W(J)*TIM
     1E))+AIMAG(SPEC(K,J+1)-SPEC(K,J))*(SIN(W(J+1)*TIME)-SIN(W(J)*TIME
     2))
   17 CONTINUE
      IF (ABS(TIME).LT.0.0001)  TIME=TIME+.0001
      FT=2.*FT/(TIME*TIME*DELF)
      FF=-REAL(SPEC(K,1))*SIN(W(1)*TIME)+AIMAG(SPEC(K,1))*COS(W(1)*TIM
     1E)+REAL(SPEC(K,NW))*SIN(W(NW)*TIME)-AIMAG(SPEC(K,NW))*COS(W(NW)*
     2TIME)
      FF=2.*FF/TIME
      FF=FT+FF
    9 PRINT 204, TIME,FF,XR(K)
    3 CONTINUE
  101 FORMAT (6I4)
  102 FORMAT (11F7.0)
  100 FORMAT (6F10.0,I3)
  103 FORMAT (3F10.0)
  105 FORMAT (3F8.0)
  200 FORMAT (*  N   M   NW  NR  NT      WO        DELF        PHIO     DE
     1LP     T1     DELT      AO      RO*)
  201 FORMAT (5I4,8F10.2)
  202 FORMAT (*   ALPHA     BETA       RHO        DEPTH       QVP       QVS
     1*)
  203 FORMAT(6F10.3,I4)
  204 FORMAT (3E10.3)

  205 FORMAT (3(E10.3,2X))
  206 FORMAT (*  RANGE       CHARGE SIZE  SHOT DEPTH*)
      END

      SUBROUTINE REFLCT(A,B,R,D,PHI,W,RPP,RPS,QP,QS,M,NW,AO,RO,INDC)
C     SUBROUTINE TO CALCULATE COMPLEX P SV PLANE
C     RETLECTION COEFFICIENTS AT ANGLES OF INCIDENCE PHI
C     TO A SERIES OF LAYERS OF DEPTH D,P AND S VELS A AND B
C     DENSITIES R, D,A,B, AND R ARE VECTORS STARTING WITH
C     UPPERMAST SOLID LAYER. PHI IS ANGLE OF INCIDENCE ON
C     UPPERMOST SOLID - LIQUID  BOUNDARY. ASSUMES TIME
C     DEPENDENCE  EXP(-IWT). ALL COEFFICIENTS REFERENCED
C     TO SEA FLOOR WHERE Z=0, Z POSITIVE DOWN. W IS ANGULAR FREQ
C     M=NO OF SOLID LAYERS,N=NO OF ANGLES,AO=WATER VEL
C     RO=WATER DENSITY,QP,QS=ATTN FACTORS SO THAT
C     VELOCITIES BECOME COMPLEX UNLESS QP,QS=0
C
C     USES METHOD OF KENNETT 1974 BSSA. 16 COEFFS PER INTERFACE
C     CALCULATER USING SUBROUTINE RPSV AND KNOTT EQUATIONS
C     THESE ARE STORED ON DISK. THESE COEFFS PHASED TO
C     Z=0=SEA FLOOR,USING SUBROUTINE PHASE
C     KENNETTS ITERATION PERFORMED FOR SUCCESSIVE
C     INTERFACES AND RESULT MULTIPLIED BY TRANS COEFF DOWN
C     THROUGH LIQUID SOLID INTERFACE
C
```

Appendix 3 (cont'd)

```
C      NO APPROXIMATIONS USED KENNETTS EQNS 30 31
C      COEFFS ARE WITH RESPECT TO DISPLACEMENT POTENTIALS
C      RESULTS RPP=P WAVE AT OBS
C              RPS=S WAVE AT OBS
C
C
       DIMENSION A(1),B(1),R(1),QP(1),QS(1),W(1)
       DIMENSION W(1)
       COMPLEX RU(2,2),RD(2,2),TU(2,2),TD(2,2),RR(2,2)
       COMPLEX RUU(2,2),RDD(2,2),TUU(2,2),TDD(2,2),RRR(2,2,2000)
       DIMENSION RPP(1),RPS(1)
       COMPLEX REM(2,2)
       COMPLEX RESS(2,2),RES(2,2),CA1,CB1,CA2,CB2,XI,A1,A2
       COMPLEX B1,B2,SA1,SB1,SA2,SB2,TPP,TPS,TPPP,Z,Z1,Z2
       DIMENSION INDC(25)
       LEVEL2,RPP,RPS,W
       XI=CMPLX(0.,1.)
C      LOOP ON ANGLES
       RES(1,1)=0.
       RES(1,2)=0.
       RES(2,1)=0.
       RES(2,2)=0.
C
       CV=SIN(PHI)/A0
       MM=M
C
C      LOOP ON LAYERS
C
C      DETERMINE IF MUST FORM COMPLEX VELOCITY FOR Q NE 0
C      DO DOWN TO 17 ONLY FOR LOWEST INTERFACE
       IF(QP(MM))10,10,11
   11  A2=A(MM)*(1.-XI/(2.*QP(MM)))
       B2=B(MM)*(1.-XI/(2.*QS(MM)))
       GO TO 20
   10  A2=A(MM)
       B2=B(MM)
C      CALCULATE SINES AND COSINES FOR LOWEST MEDIA SQRTS POSITIVE
   20  SA2=A2*CV
       SB2=B2*CV
       IF (1.-CABS(SA2*SA2)) 12,13,13
   13  CA2=CSQRT(1.-SA2*SA2)
       GO TO 14
   12  CA2=XI*CSQRT(SA2*SA2-1.)
   14  IF (1.-CABS(SB2*SB2)) 15,16,16
   16  CB2=CSQRT(1.-SB2*SB2)
       GO TO 17
   15  CB2=XI*CSQRT(SB2*SB2-1.)
   17  MM=MM-1
       IF(MM.EQ.0) GO TO 71
       IF(QP(MM)) 18,18,19
   19  A1=A(MM)*(1.-XI/(2.*QP(MM)))
       B1=B(MM)*(1.-XI/(2.*QS(MM)))
       GO TO 21
   18  A1=A(MM)
       B1=B(MM)
C
C      CALCULATE SINES AND COSINES FOR MEDIA 1
   21  SA1=CV*A1
       SB1=CV*B1
       IF (1.-CABS(SA1*SA1)) 22,23,23
   23  CA1=CSQRT(1.-SA1*SA1)
       GO TO 24
   22  CA1=XI*CSQRT(SA1*SA1-1.)
   24  IF(1.-CABS(SB1*SB1)) 25,26,26
   26  CB1=CSQRT(1.-SB1*SB1)
       GO TO 27
   25  CB1=XI*CSQRT(SB1*SB1-1.)
   27  CONTINUE
       CALL RPSV (CV,A1,A2,B1,B2,R(MM),R(MM+1),RUU,RDD,TUU,TDD,CA1,CB1,
      1CA2,CB2)
```

Appendix 3 (cont'd)

```
C     ABOVE SUBROUTINE CALCULATES REFL ,TRANS COEFFS FOR ONE INTERFACE
C     BETWEEN MEDIA 1 AND 2. RETURNS MATRICES OF COEFFS RU,RD,TU,TD
C
C     LOOP ON FREQ AS PHASES ARE CALCULATED Z=0 IS SEA FLOOR
C     CALCULATE COEFFS PHASED TO SEA FLOOR
      DO 2 J=1,NW
      WW=W(J)
      DO 3 I=1,2
      DO 3 K=1,2
      RU(I,K)=RUU(I,K)
      RD(I,K)=RDD(I,K)
      TU(I,K)=TUU(I,K)
      TD(I,K)=TDD(I,K)
    3 RR(I,K)=RRF(I,K,J)
      CALL PHASE (RU,RD,TU,TD,CA1,CA2,CB1,CB2,D(MM+1),D(MM),XI,WW,A1,A
     12,B1,B2,M),RETURNS (70)
C     IF LOWEST INTERFACE GO TO 31
      IF (MM+1-M) 30,31,31
C     CALCULATE INTERATION AS IN KENNETT
C     FIRST CALC TU(J-1)RD(J)(I-RU(J-1)RD(J))-1*TD(J-1)
C     USING SUBROUTINE FOR 2S2 COMPLEX MATRICES MULTC AND INVR FOR INVERSION
   30 CALL MULTC(RU,RR,RES)
      IND=INDC(MM)
      IF (IND.NE.0) GO TO 35
      RES(1,1)=1.-RES(1,1)
      RES(1,2)=-RES(1,2)
      RES(2,1)=-RES(2,1)
      RES(2,2)=1.-RES(2,2)
      CALL INVR(RES,RESS)
      GO TO 36
   35 DO 38 JJ=1,2
      DO 38 II=1,2
      REM(II,JJ)=RES(II,JJ)
   38 RESS(II,JJ)=RES(II,JJ)
      IF (IND.EQ.1) GO TO 39
      DO 37 KK=2,IND
      CALL MULTC (RES,REM,REM)
      DO 40 II=1,2
      DO 40 JJ=1,2
   40 RESS(II,JJ)=REM(II,JJ)+RESS(II,JJ)
   37 CONTINUE
   39 CONTINUE
      RESS(1,1)=1.+RESS(1,1)
      RESS(2,2)=1.+RESS(2,2)
   36 CONTINUE
      CALL MULTC(RESS,TD,RES)
      CALL MULTC(RR,RES,RESS)
      CALL MULTC(TU,RESS,RES)
C     TOTAL COEFF IS
C
   31 RRF(1,1,J)=RD(1,1)+RES(1,1)
      RRF(1,2,J)=RD(1,2)+RES(1,2)
      RRF(2,1,J)=RD(2,1)+RES(2,1)
      RRF(2,2,J)=RD(2,2)+RES(2,2)
   70 CONTINUE
    2 CONTINUE
C     SWITCH MEDIA 2 FOR MEDIA 1
      SA2=SA1
      SB2=SB1
      CA2=CA1
      CB2=CB1
      A2=A1
      B2=B1
      GO TO 17
   71 CONTINUE
C     CALCULATION ON TRANS COEFFS DOWN FROM LIQUID TO SOLID
C     AFTER BREKHONSKI P 31
      R2=R(1)
      SA1=SIN(PHI)
      CA1=COS(PHI)
      SQ=SQRT(REAL(SA1))
```

```
      Z=R0*A0/CA1
      Z1=R2*A2/CA2
      Z2=R2*B2/CB2
      TPPP=Z1*((1.-2.*(SB2**2))**2)+Z2**4.*(CB2*SB2)**2+Z
      TPP=(R0/R2)*(2.*Z1*(1.-2.*SB2**2))/TPPP
      TPS=-(R0/R2)*4.*Z2*SB2*CB2/TPPP
C     MULTIPLY TO OBTAIN TOTAL REFL COEFFS RRP,RPS,PHASED TO SEA FLOOR
C
C     LOOP ON FREQ AGAIN AS MULT TOTAL COEFFS BY TRANS COEFFS DOWN
      DO 1 J=1,NW
      RRF(1,1,J)=RRF(1,1,J)*TPP+RRF(1,2,J)*TPS
      RRF(2,1,J)=RRF(2,1,J)*TPP+RRF(2,2,J)*TPS
      RRF(2,2,J)=(RRF(1,1,J)*CA1-XI*RRF(2,1,J)*SA1*SA1*W(J)/A0)*SQ
      RPP(J)=CABS(RRF(2,2,J))
      RPS(J)=ATAN2(AIMAG(RRF(2,2,J)),REAL(RRF(2,2,J)))
    1 CONTINUE
      RETURN
      END

      SUBROUTINE RPSV(CV,A1,A2,B1,B2,R1,R2,RU,RD,TU,TD,CA1,CB1,CA2,CB2)
      COMPLEX CA1,CB1,CA2,CB2
      COMPLEX A1,A2,B1,B2,RU(2,2),RD(2,2),TU(2,2),TD(2,2)
      COMPLEX V(4),P(4),Q,X,Y,Z,D
      COMPLEX R(4,4)
      COMPLEX CVQ
      Q=2.*(R2*(B2**2)-R1*(B1**2))
      CVQ=(CV**2)*Q
      X=R2-CVQ
      Y=R1+CVQ
      Z=R2-R1-CVQ
      V(1)=A1
      V(2)=B1
      V(3)=A2
      V(4)=B2
      P(1)=CA1
      P(2)=CB1
      P(3)=CA2
      P(4)=CB2
      D=A1*A2*B1*B2*(CV**2)*(Z**2)+A2*B2*P(1)*P(2)*(X**2)
      D=D+A1*B1*P(3)*P(4)*(Y**2)
      D=D+R1*R2*(B1*A2*P(1)*P(4)+A1*B2*P(2)*P(3))+((Q*CV)**2)*P(1)*P(2
     1)*P(3)*P(4)
      R(1,1)=-1.+(2.*P(1)*(A2*B2*P(2)*(X**2)+B1*A2*R1*R2*R(4)+((Q*CV)*
     1*2)*P(2)*P(3)*P(4)))/D
      R(1,2)=-2.*A1*CV*P(1)*(Q*P(3)*P(4)*Y-A2*B2*X*Z)/D
      R(1,3)=2.*A1*R1*P(1)*(B2*P(2)*X+B1*P(4)*Y)/D
      R(1,4)=-2.*A1*R1*CV*P(1)*(Q*P(2)*P(3)-B1*A2*Z)/D
      R(2,2)=1.-(2.*P(2)*(A2*B2*P(1)*(X**2)+A1*B2*R1*B2*P(3)+((Q*CV)**
     1*2)*P(1)*P(3)*P(4)))/D
      R(2,3)=2.*B1*R1*CV*P(2)*(Q*P(1)*P(4)-A1*B2*Z)/D
      R(2,4)=2.*B1*R1*P(2)*(A1*P(3)*Y+A2*P(1)*X)/D
      R(3,3)=-1.+(2.*P(3)*(A1*B1*P(4)*(Y**2)+A1*B2*R1*R2*P(2)+((Q*CV)*
     1*2)*P(1)*P(2)*P(4)))/D
      R(3,4)=2.*A2*CV*P(3)*(Q*P(1)*P(2)*X+A1*B1*Y*Z)/D
      R(4,4)=1.-(2.*P(4)*(A1*B1*P(3)*(Y**2)+B1*A2*R1*B2*P(1)+((Q*CV)**
     2*2)*P(1)*P(2)*P(3)))/D
      R(2,1)=P(2)*V(2)*R(1,2)/(P(1)*V(1))
      R(3,1)=P(3)*V(3)*R2*R(1,3)/(P(1)*V(1)*R1)
      R(3,2)=P(3)*V(3)*R2*R(2,3)/(P(2)*V(2)*R1)
      R(4,1)=P(4)*V(4)*R2*R(1,4)/(P(1)*V(1)*R1)
      R(4,2)=P(4)*V(4)*R2*R(2,4)/(P(2)*V(2)*R1)
      R(4,3)=P(4)*V(4)*R(3,4)/(P(3)*V(3))
      R(2,1)=-R(2,1)
      R(2,2)=-R(2,2)
      R(3,4)=-R(3,4)
      R(4,4)=-R(4,4)
      R(2,3)=-R(2,3)
      R(1,4)=-R(1,4)
      DO 10 I=1,2
      DO 10 J=1,4
```

Appendix 3 (cont'd)

```
      IF (J.LE.2) GO TO 11
      TD(J-2,I)=R(I,J)*V(J)/V(I)
      GO TO 10
   11 RD(J,I)=R(I,J)*V(J)/V(I)
   10 CONTINUE
      SUBROUTINE PHASE (RU,RD,TU,TD,CA1,CA2,CB1,CB2,D2,D1,XI,W,A1,A2,B
     *1,B2,M),RETURNS(A)
      DIMENSION IND(4)
      COMPLEX PHI(4),XI,PHAS,RU(2,2),RD(2,2),TU(2,2),TD(2,2),A1,A2,B1,
     *B2,CA1,CB1,CA2,CB2
      DO 2 J=1,4
    2 IND(J)=1
      PHI(1)=-XI*CA2*W/A2
      PHI(2)=-XI*CB2*W/B2
      PHI(3)=-XI*CA1*W/A1
      PHI(4)=-XI*CB1*W/B1
      DO 1 I=1,4
      IF (REAL(PHI(I))*(D2-D1).GT.20.) IND(I)=0
    1 CONTINUE
C     FIND IF ALL CRITICAL ANGLES EXCEEDED
      JJ=MAX0(IND(1),IND(2),IND(3),IND(4))
C     IF ALL EXCEEDED DROP INTERFACE AND RETURN TO DO NEXT INTERFACE
      IF (JJ.EQ.0) GO TO 200
      DO 100 I=1,4
  100 PHI(I)=PHI(I)*D2
      DO 101 K=1,2
      DO 101 L=1,2
      RU(K,L)=IND(K)*IND(L)*RU(K,L)*CEXP(PHI(K)+PHI(L))
      RD(K,L)=IND(K+2)*IND(L+2)*RD(K,L)*CEXP(-(PHI(K+2)+PHI(L+2)))
      PHAS=PHI(L)-PHI(K+2)
      TU(K,L)=IND(K+2)*IND(L)*TU(K,L)*CEXP(PHAS)
  101 TD(L,K)=IND(K+2)*IND(L)*TD(L,K)*CEXP(PHAS)
      RETURN
  200 M=M-1
      RETURN A
      END

      DO 12 I=1,2
      DO 12 J=1,4
      IF (J.GE.3) GO TO 14
      TU(J,I)=R(I+2,J)*V(J)/V(I+2)
      GO TO 12
   14 RU(J-2,I)=R(I+2,J)*V(J)/V(I+2)
   12 CONTINUE
      RETURN
      END

      SUBROUTINE SPLAT (W,D,BB,XB,FREQ,NL,A)
      DIMENSION FREQ(150)
      COMPLEX XB(150)
      COMPLEX BB(150),XI,CA,CB,CC,SO
      TWPI=2.*3.1415926
      XI=CMPLX(0.,1.)
C     CALCULATION OF SOURCE *INSTRU RESPONSE
C     THIS PROGRAM TAKES INSTRU RESP =BB AT FREWS=FREQ CALCULATES EFFECT OF
C     SOURCE INCLUDING  SURFACE REFLECTION AND TWO BUBBLE PULSES
C     MULTIPLIES INSTRU *SOURCE RESP =TOTAL RESP
C     SHOCH WAVE + BUBBLES APPROX BY IMPULSES OVER FREQ RANGE
C     OF INTEREST IE UP TO 17 HZ
C     A=RADIUS FOR CLLCULATIONS AROUND 10 M
C     W=CHARGE SIZE IN LBS
C     D = DEPTH IN M
C     NL VALUES OF XB=INSTRU RESP ON INPUT,BB = TOTAL RESP ON OUTPUT
C
C     SEE WESTON 1960
      WT=W**.3333
      HT=3.2808*D
      AT=3.2808*A
      TR=(2.*D/1500.)
      PER=4.36*WT/((HT+33.)**(5./6.))
```

Appendix 3 (cont'd)

```
      PMAX=3450.*(WT/AT)
      TCB=9.58/(3450.*2.*((HT+33.)**(1./6.)))
      XIMP1=PMAX*2.*TCB
C     SECOND BUBBLE
      XIMP2=XIMP1/2.49
      PER2=.72*PER
C     SHOCK WAVE
      PS=2.16*(10**4)*((WT/AT)**1.13)
      TCS=58.*WT*((WT/AT)**(-.24))
C     CALC OF SOURCE SPECTRUM AND TOTAL SPECTRUM
      DO 10 L=1,NL
      CA=1.-CEXP(XI*TUPI*FREQ(L)*TR)
      CB=CEXP(XI*TUPI*FREQ(L)*PER)
      CC=CEXP(XI*TUPI*FREQ(L)*PER2)
      SO=PS*TCS*CA+XIMP1*CA*CB+XIMP2*CA*CC
      BB(L)=SO*XB(L)
      PRINT 100, SO,BB(L),FREQ(L)
   10 CONTINUE
  100 FORMAT (5(E12.5,2X))
      RETURN
      END

      SUBROUTINE MULTC(A,B,C)
      COMPLEX A(2,2),B(2,2),C(2,2)
      C(1,1)=A(1,1)*B(1,1)+A(1,2)*B(2,1)
      C(1,2)=A(1,1)*B(1,2)+A(1,2)*B(2,2)
      C(2,1)=A(2,1)*B(1,1)+A(2,2)*B(2,1)
      C(2,2)=A(2,1)*B(1,2)+A(2,2)*B(2,2)
      RETURN
      END
```